Overview of STING-Associated Vasculopathy with Onset in Infancy (SAVI) Among 21 Patients

Marie-Louise Frémond, Alice Hadchouel, Laureline Berteloot, Isabelle Melki, Violaine Bresson, Laura Barnabei, Nadia Jeremiah, Alexandre Belot, Vincent Bondet, Olivier Brocq, et al.

Overview of STING-Associated Vasculopathy with Onset in Infancy (SAVI) Among 21 Patients

Article *in* The Journal of Allergy and Clinical Immunology In Practice · November 2020

DOI: 10.1016/j.jaip.2020.11.007

CITATIONS
99

READS
256

44 authors, including:

Marie-Louise Frémond
Hôpital Universitaire Necker
102 PUBLICATIONS **3,271** CITATIONS
SEE PROFILE

Berteloot Laureline
Hôpital Universitaire Necker
101 PUBLICATIONS **1,993** CITATIONS
SEE PROFILE

Isabelle Melki
Institut Imagine
136 PUBLICATIONS **3,108** CITATIONS
SEE PROFILE

Laura Barnabei
IOR Institute of Oncology Research
32 PUBLICATIONS **3,308** CITATIONS
SEE PROFILE

Original Article

Overview of STING-Associated Vasculopathy with Onset in Infancy (SAVI) Among 21 Patients

Marie-Louise Frémond, MD, PhD[b,c], Alice Hadchouel, MD, PhD[a,d,e], Laureline Berteloot, MD[f], Isabelle Melki, MD, PhD[b,c,g], Violaine Bresson, MD[h], Laura Barnabei, PhD[i], Nadia Jeremiah, PhD[j], Alexandre Belot, MD, PhD[k,l], Vincent Bondet, MSc[m], Olivier Brocq, MD[n], Damien Chan, MD[o], Rawane Dagher, MD[p], Jean-Christophe Dubus, MD, PhD[q], Darragh Duffy, PhD[m], Séverine Feuillet-Soummer, MD, PhD[r], Mathieu Fusaro, PharmaD, MSc[s,t], Marco Gattorno, MD[u], Antonella Insalaco, MD[v], Eric Jeziorski, MD[w], Naoki Kitabayashi, MSc[b], Mireia Lopez-Corbeto, MD[x], Françoise Mazingue, MD[y], Marie-Anne Morren, MD[z,aa], Gillian I. Rice, PhD[bb], Jacques G. Rivière, MD[cc,dd,ee], Luis Seabra, MSc[b], Jérôme Sirvente, MD[ff], Pere Soler-Palacin, MD, PhD[cc,dd,ee,gg], Nathalie Stremler-Le Bel, MD[q], Guillaume Thouvenin, MD[hh], Caroline Thumerelle, MD[ii], Eline Van Aerde, MD[z], Stefano Volpi, MD, PhD[u], Sophie Willcocks, MD[jj], Carine Wouters, MD, PhD[c,kk,ll], Sylvain Breton, MD[f], Thierry Molina, MD, PhD[a,mm], Brigitte Bader-Meunier, MD[c,i], Despina Moshous, MD, PhD[c,nn], Alain Fischer, MD, PhD[c,oo,pp], Stéphane Blanche, MD[a,c], Frédéric Rieux-Laucat, PhD[j,*], Yanick J. Crow, MD, PhD[b,qq,*], and Bénédicte Neven, MD, PhD[c,i]

Paris, Marseille, Lyon, Le Plessis-Robinson, Montpellier, and Lille, France; Monaco, Monaco; Adelaide (South Australia) and Brisbane (Queensland), Australia; Jbeil, Lebanon; Genova and Rome, Italy; Barcelona and Bellaterra (Catalonia), Spain; Leuven, Belgium; Lausanne, Switzerland; and Manchester and Edinburgh, United Kingdom

What is already known about this topic? STING-associated vasculopathy with onset in infancy, caused by gain-of-function mutations in *STING1*, is typically characterized by early-onset systemic inflammation, skin vasculopathy, and interstitial lung disease. Janus kinase (JAK) inhibitors are promising treatment.

What does this article add to our knowledge? Lung disease was constant, leading to early and insidious development of fibrosis, and polyarthritis (including destructive form) with positive rheumatoid factor frequently occurs. Overlapping features with other monogenic interferonopathies may arise. Treatment with ruxolitinib improved clinical features of the disease.

How does this study impact current management guidelines? The extension of STING-associated vasculopathy phenotype warrants careful clinical and genetic screening of patients with apparently isolated skin, lung, or joint inflammation, in particular with early onset, and in the presence of autoantibodies or memory CD8 lymphopenia. Early diagnosis is needed to maximize treatment benefit with JAK inhibitors.

[a]Université de Paris, Paris, France
[b]Université de Paris, Imagine Institute, Laboratory of Neurogenetics and Neuroinflammation, Paris, France
[c]Pediatric Hematology-Immunology and Rheumatology Department, Hôpital Necker-Enfants Malades, AP-HP Centre Université de Paris, Paris, France
[d]Pediatric Pulmonology Department, Hôpital Necker-Enfants Malades, AP-HP Centre Université de Paris, Paris, France
[e]INEM, INSERM U1151, Paris, France
[f]Pediatric Radiology Department, Hôpital Necker-Enfants Malades, AP-HP Centre Université de Paris, Paris, France
[g]General Pediatrics—Infectious Diseases and Internal Medicine Department, Hôpital Robert Debré, AP-HP Nord-Université de Paris, Paris, France
[h]Pediatric Emergency Department, Hôpital de la Timone, AP-HM, Centre Hospitalier Universitaire de Marseille, Marseille, France
[i]Université de Paris, Imagine Institute, Laboratory of Immunogenetics of Pediatric Autoimmunity, INSERM UMR 1163, Paris, France
[j]Immunity and Cancer Department, Institut Curie, PSL Research University, Institut National de la Santé et de la Recherche Médicale U932, Paris, France
[k]Pediatric Rheumatology, Nephrology and Dermatology Department, Hospices Civils de Lyon, Lyon, France
[l]CIRI, Centre International de Recherche en Infectiologie, INSERM, U1111, CNRS UMR5308, Ecole Normale Supérieure de Lyon, Université Lyon 1, Lyon, France
[m]Translational Immunology Lab, Institut Pasteur, Paris, France
[n]Rheumatology Department, Centre Hospitalier Princesse Grace, Monaco, Monaco
[o]Pediatric Allergy and Immunology Department, Women's and Children's Hospital, Adelaide, South Australia, Australia
[p]Department of Pediatrics, Notre Dame des Secours University Hospital, Jbeil, Lebanon
[q]Pediatric Pulmonology Department, Hôpital de la Timone, AP-HM, Centre Hospitalier Universitaire de Marseille, Marseille, France
[r]Department of Thoracic and Vascular Surgery and Heart-Lung Transplantation, Marie-Lannelongue Hospital, Paris-Sud University, Le Plessis-Robinson, France
[s]Study Center for Primary Immunodeficiencies, Hôpital Necker-Enfants Malades, AP-HP Centre Université de Paris, Paris, France
[t]Université de Paris, Imagine Institute, Laboratory of Lymphocyte Activation and Susceptibility to EBV Infection, INSERM UMR 1163, Paris, France

Abbreviations used
AGS- Aicardi-Goutières syndrome
ANCA- Antineutrophil cytoplasmic antibodies
BAL- Bronchoalveolar lavage
CID- Combined immunodeficiency
CSF- Cerebrospinal fluid
CT- Computed tomography
ICC- Intracranial calcification
IFN- Interferon
ILD- Interstitial lung disease
ISG- Interferon-stimulated gene
JAK- Janus kinase
JIA- Juvenile idiopathic arthritis
RF- Rheumatoid factor
SAVI- STING-associated vasculopathy with onset in infancy
SD- Standard deviation
STING- Stimulator of Interferon Genes

BACKGROUND: Gain-of-function mutations in *STING1* underlie a type I interferonopathy termed SAVI (STING-associated vasculopathy with onset in infancy). This severe disease is variably characterized by early-onset systemic inflammation, skin vasculopathy, and interstitial lung disease (ILD).
OBJECTIVE: To describe a cohort of patients with SAVI.
METHODS: Assessment of clinical, radiological and immunological data from 21 patients (17 families) was carried out.
RESULTS: Patients carried heterozygous substitutions in *STING1* previously described in SAVI, mainly the p.V155M. Most were symptomatic from infancy, but late onset in adulthood occurred in 1 patient. Systemic inflammation, skin vasculopathy, and ILD were observed in 19, 18, and 21 patients, respectively. Extensive tissue loss occurred in 4 patients. Severity of ILD was highly variable with insidious progression up to end-stage respiratory failure reached at teenage in 6 patients. Lung imaging revealed early fibrotic lesions. Failure to thrive was almost constant, with severe growth failure seen in 4 patients. Seven patients presented polyarthritis, and the phenotype in 1 infant mimicked a combined immunodeficiency. Extended features reminiscent of other interferonopathies were also found, including intracranial calcification, glaucoma and glomerular nephropathy. Increased expression of interferon-stimulated genes and interferon α protein was constant. Autoantibodies were frequently found, in particular rheumatoid factor. Most patients presented with a T-cell defect, with low counts of memory CD8+ cells and impaired T-cell proliferation in response to antigens. Long-term follow-up described in 8 children confirmed the clinical benefit of ruxolitinib in SAVI where the treatment was started early in the disease course, underlying the need for early diagnosis. Tolerance was reasonably good.
CONCLUSION: The largest worldwide cohort of SAVI patients yet described, illustrates the core features of the disease and extends the clinical and immunological phenotype to include overlap with other monogenic interferonopathies. © **2020 American Academy of Allergy, Asthma & Immunology (J Allergy Clin Immunol Pract 2020;■:■-■)**

Key words: *Stimulator of interferon genes;* STING1*; Type I interferonopathy; Interstitial lung disease; Vasculopathy; Polyarthritis; Lymphopenia; JAK inhibitors*

Gain-of-function mutations in *STING1*, encoding STING (Stimulator of Interferon Genes), have been described to cause an autoinflammatory syndrome termed SAVI (STING-associated vasculopathy with onset in infancy).[1,2] This disease belongs to a newly defined class of disorders referred to as the type I

[u]Center for Autoinflammatory Diseases and Immunodeficiencies, IRCCS Giannina Gaslini Institute, Genova, Italy
[v]Pediatric Rheumatology Unit, IRCCS Ospedale Pediatrico Bambino Gesù, Rome, Italy
[w]Pediatrics Department, Centre Hospitalier Universitaire de Montpellier, Montpellier, France
[x]Pediatric Rheumatology Unit, Rheumatology Department, Hospital Universitari Vall d'Hebron, Vall d'Hebron Barcelona Hospital Campus, Barcelona, Catalonia, Spain
[y]Pediatric Hematology Department, Centre Hospitalier Universitaire de Lille, Lille, France
[z]Dermatology Department, University Hospitals Leuven, Leuven, Belgium
[aa]Department of Pediatrics and Dermatol-Venereology, University Hospital Lausanne and University of Lausanne Pediatric Dermatology Unit, Lausanne, Switzerland
[bb]Division of Evolution and Genomic Sciences, School of Biological Sciences, Faculty of Biology, Medicine and Health, University of Manchester, Manchester Academic Health Science Centre, Manchester, United Kingdom
[cc]Infection in Immunocompromised Pediatric Patients Research Group, Vall d'Hebron Institut de Recerca (VHIR), Hospital Universitari Vall d'Hebron, Barcelona, Catalonia, Spain
[dd]Pediatric Infectious Diseases and Immunodeficiencies Unit, Hospital Universitari Vall d'Hebron, Barcelona, Catalonia, Spain
[ee]Jeffrey Modell Diagnostic and Research Center for Primary Immunodeficiencies, Barcelona, Spain
[ff]Internal Medicine Department, Hôpital Saint-Eloi, Centre Hospitalier Universitaire de Montpellier, Montpellier, France
[gg]Universitat Autònoma de Barcelona, Bellaterra, Catalonia, Spain
[hh]Pediatric Pulmonology Department and Reference Center for Rare Lung Disease RespiRare, Trousseau University Hospital, AP-HP Sorbonne Université, Paris, France
[ii]Pediatric Pneumology Department, Hôpital Jeanne de Flandre, CHRU Lille, Lille, France
[jj]Pediatric Immunology and Allergy Service, Queensland Children's Hospital, Children's Health Queensland, Brisbane, Queensland, Australia
[kk]Pediatrics Department, University Hospitals Leuven, Leuven, Belgium
[ll]Department of Immunology and Microbiology—Childhood Immunology University of Leuven, Leuven, Belgium
[mm]Pathology Department, Hôpital Necker-Enfants Malades, AP-HP Centre Université de Paris, Paris, France
[nn]Université de Paris, Imagine Institute, Laboratory of Genome Dynamics in the Immune System, INSERM UMR 1163, Paris, France
[oo]Université de Paris, Imagine Institute, INSERM UMR 1163, Paris, France
[pp]Collège de France, Paris, France
[qq]Centre for Genomic and Experimental Medicine, MRC Institute of Genetics and Molecular Medicine, University of Edinburgh, Edinburgh, United Kingdom
* These authors contributed equally to this work.

Sources of funding are the Institut National de la Santé et de la Recherche Médicale, the European Research Council, and the National Research Agency (ANR) M.-L. Frémond received a grant from the Institut National de la Santé et de la Recherche Médicale (reference: 000427993). Y.J. Crow acknowledges the European Research Council (GA309449 and 786142-E-T1IFNs), and a state subsidy managed by the National Research Agency (France) under the 'Investments for the Future' programme bearing the reference ANR-10-IAHU-01. Y.J. Crow and D.Duffy acknowledge the National Research Agency (France)(grant CE17001002).
Conflicts of interest: The authors declare that they have no relevant conflicts of interest.
Received for publication July 29, 2020; revised October 30, 2020; accepted for publication November 3, 2020.
Available online ■■

Corresponding authors: Bénédicte Neven, MD, PhD, Pediatric Hematology-Immunology and Rheumatology Department, Hôpital Necker-Enfants Malades, 149 rue de Sèvres, 75015 Paris, France. (E-mail: benedicte.neven@aphp.fr); Or: Yanick J. Crow, MD, PhD, MRC Institute of Genetics and Molecular Medicine, The University of Edinburgh, Crewe Road, Edinburgh EH4 2XU, United Kingdom. (E-mail: yanickcrow@mac.com).

2213-2198

https://doi.org/10.1016/j.jaip.2020.11.007

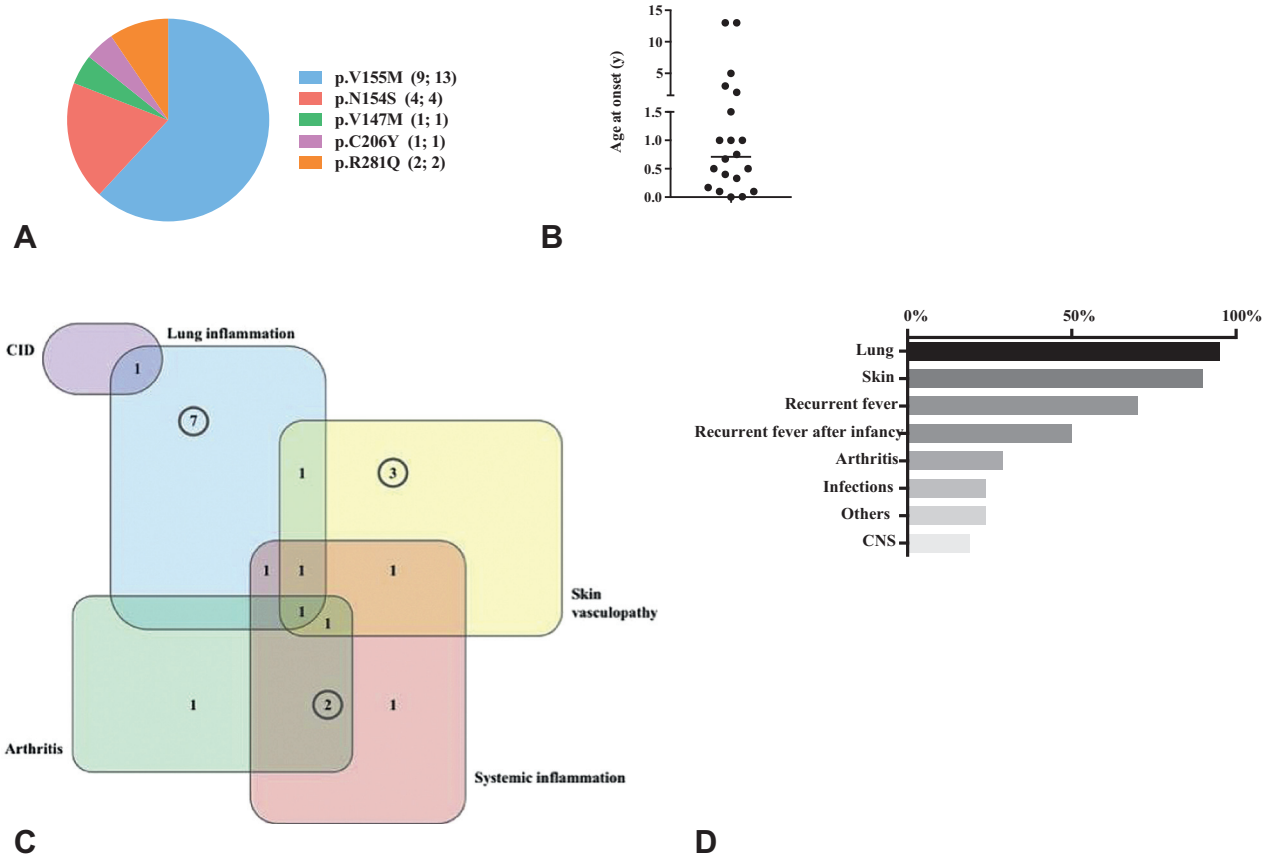

FIGURE 1. Genetic characteristics, clinical onset, and disease course of the patients. **A**, Numbers of patients carrying the heterozygous mutations, p.V147M, p.N154S, p.V155M, p.C206Y, and p.R281Q in *STING1*. Numbers in the parentheses refer to the number of families identified and mutation carriers, respectively. **B**, Distribution of age at onset. Most patients were symptomatic below the age of 1 year. **C**, Specific and overlapping features present at onset, including lung inflammation, skin vasculopathy, systemic inflammation (referring to recurrent fever and/or increased inflammatory markers), arthritis, and combined immunodeficiency (CID). **D**, Frequency (expressed as a percentage) of associated features in the cohort during the course of the disease. "Others" refers to myositis, hepatitis, kidney involvement, pericarditis, and glaucoma. "CNS," central nervous system, refers to neurological symptoms or lymphocytic meningitis.

interferonopathies[3,4] and is variably characterized by early-onset systemic inflammation with fever, a severe skin vasculopathy leading in some cases to extensive tissue loss, and interstitial lung disease (ILD) resulting in pulmonary fibrosis and end-stage respiratory failure.[1,2,5-24] SAVI is rare—with 52 patients in 37 families reported so far[1,2,5-24]—and principally occurs *de novo*, although autosomal dominant inheritance[2,11,20,21] has been recorded. Recently, patients with activating homozygous mutations of *STING1* have been described, highlighting the genetic complexity of this disease.[22] The initially described phenotype[1,2] was subsequently expanded to include apparently isolated lung fibrosis[7] and isolated familial lupus chilblain (stably inherited across 4 generations).[11] Other features include myositis, arthritis, and recurrent bacterial infections.[1,10] STING gain-of-function is associated with enhanced constitutive type I interferon (IFN) signaling, as assessed by increased phosphorylation of STAT1 in T lymphocytes, increased transcription of IFN-stimulated genes (ISGs) by blood circulating cells of patients,[1,2] and elevated IFNα protein in circulating monocytes and plasmacytoid dendritic cells.[25] SAVI is minimally responsive to conventional immunosuppressive therapies, and thus associated with marked childhood morbidity and increased mortality.[1,2,5-21] In 2016, we reported improvement of cutaneous and pulmonary phenotype of the disease under ruxolitinib, a Janus kinase (JAK)1/2 inhibitor in 3 children with SAVI.[26] This experience was confirmed by further reports using either JAK1/2 inhibitors (ruxolitinib, baricitinib), or tofacitinib, a JAK1/3 inhibitor.[16,27]

Herein, we describe the largest worldwide cohort of patients carrying *STING1*-activating mutations, thereby providing an extended clinical and immunological phenotypic description of SAVI.

METHODS

Cohort of patients

Twenty-one patients with genetically confirmed SAVI, of whom 12 have been previously reported,[2,5,7,10] were included in this retrospective study. They were recruited from institutions in France, Monaco, Belgium, Italy, Spain, Lebanon, and Australia (the names of the institutions are given in this article's Online Repository at www.jaci-inpractice.org). Clinical characteristics at onset and during follow-up were recorded. Biological parameters such as inflammatory

TABLE I. Comparison of the present patient cohort with previously reported patients

	Our cohort (n = 21)	Literature[1,6,8-15,17-24],* (n = 40)	Total (n = 61)
Last status, n (%)	Alive: 17 (81)	Alive: 32 (80)	Alive: 49 (80)
Median age at the time of reporting (y)	8 (0.6-65)	14** (1-86)	11.5 (0.6-86)
Median clinical onset (y)	0.71† (0-13)	0.17†† (0-16)	0.37 (0-16)
Onset before 6 mo, n (%)	10 (50)	27†† (68)	37†† (62)
Systemic involvement, n (%)			
Failure to thrive	15† (75)	26/34 (76)	41/55† (75)
Recurrent fevers	14† (70)	14/39 (36)	28/60 (47)
Systemic inflammation	18† (90)	25/39 (64)	43/60 (72)
Cutaneomucosal lesions, n (%)			
Rash	18 (86)	22/37 (59)	40/58 (69)
Ulcers	11 (52)	20/37 (54)	31/58 (53)
Extensive tissue loss	4 (19)	5/37 (14)	9/58 (16)
Nasal perforation	3 (14)	11/37 (30)	14/58 (24)
Lung features, n (%)			
ILD	21 (100)	25/37 (68)	46/58 (79)
Lung fibrosis	16 (76)	7/29 (24)	23/50 (46)
Musculoskeletal involvement, n (%)			
Arthritis	7‡ (33)	7/40 (18)	14/61 (23)
Arthralgia without arthritis	3 (14)	3/40 (8)	6/61 (10)
Myositis	1 (5)	3/40 (8)	4/61 (7)
Infections, n (%)			
	5 (24)	12/40 (32)	17/61 (28)
Cerebral features, n or n (%)			
Symptoms	Spastic diplegia (n = 1) Seizures (n = 1)	Cerebrovascular involvement with hallucinations and headaches[19] (n = 1)	3/61 (5)
ICC	3§ of 12	NR	3§ of 12
Other symptoms, n			
	Glaucoma (n = 1) Hepatitis (n = 1) Glomerular kidney disease‖ (n = 2)	Thyroiditis[20] (n = 1) Focal segmental glomerulosclerosis and thrombotic microangiopathy[24] (n = 1)	Glaucoma (n = 1) Hepatitis (n = 1) Thyroiditis (n = 1) Kidney disease (n = 3)
Autoantibodies, n/n of pts assessed			
ANA	15/21	20/35	35/56
Anti-DNA	4/19	2/18	6/37
ANCA	15/21	7/NR	22/21+NR
RF	11/19	6/11	17/30
Treatment and procedures, n (%)			
Steroids	17† (81)	24/35 (69)	41/56† (73)
DMARDs	15† (71)	16/34 (47)	31/56† (55)
Biologics	10† (50) Anticytokines: 7 • anti-TNFα: 5 • anti-IL1: 2 • anti-IL6: 3	11/34 (32) Anticytokines: 7 • anti-TNFα: 5 • anti-IL1: 2 • anti-IL6: 2	21/56† (38) Anticytokines: 14 • anti-TNFα: 10 • anti-IL1: 4 • anti-IL6: 5
JAK inhibitors	17¶ (81)	21/33 (64)	38/54 (70)
Lung transplantation	1# (5)	1[21]	2

ANA, Antinuclear antibodies; *ANCA*, antineutrophil cytoplasmic antibodies; *anti-DNA*, anti−double-stranded DNA antibodies; *DMARD*, disease-modifying antirheumatic drug; *ICC*, intracranial calcification; *ILD*, interstitial lung disease; *JAK*, Janus kinase; *mo*, months; *n*, number of patients; *NR*, not recorded; *pts*, patients; *RF*, rheumatoid factor; *y*, year.

*The patients of our cohort that have been previously published[2,5,7,10,16] are not included in the "literature patients."

†Not recorded for 1 patient (P4) but onset occurred in adulthood.

‡Among whom 2 patients with severe joint deformities.

§In the globi pallidi.

‖Hypertension with microscopic hematuria and mild proteinuria (no kidney biopsy performed) and glomerulonephritis.

¶Treatment initiated after end point data collection.

#After end point data collection, 2 patients (P7 and P12) have been programmed for lung transplantation.

**Not recorded for 3 patients.

††Not recorded for 1 patient.[24]

markers, autoantibodies, and immunological status were collected. The end point for data collection was censored at the last follow-up (May 2019), death, or initiation of the JAK1/2 inhibitor ruxolitinib.

A monocentric assessment of IFN biomarkers was determined by studying the expression of ISGs[28] in peripheral blood, measurement of IFNα in serum or plasma using ultrasensitive Simoa digital ELISA,[25] and STAT1 phosphorylation in patients' cells.[26]

Study approval

The study was approved by the Comité de protection des personnes Ile de France II and the French advisory committee on data processing in medical research. Written informed consent was obtained for pictures appearing in the paper.

Thoracic imaging analyses

Dr Laureline Berteloot (Pediatric Radiology, Necker Hospital, Paris, France) centrally reviewed the chest computed tomography (CT) scans of 16 patients of the cohort. The description of this standardized analysis is provided in this article's Online Repository at www.jaci-inpractice.org. The presence of honeycombing and/or traction bronchiectasis and/or decreased lung volume radiologically defined fibrosis.

Response to JAK inhibition

In addition to the descriptive cohort, treatment with a JAK1/2 inhibitor is reported in 8 patients. Disease scores,[26] IFN biomarkers, inflammatory markers, and chest CT scans (when available) were assessed before and at the last follow-up.

Statistics

Data were expressed as median (minimal-maximal range). Analyses were performed with PRISM software (v6 for Macintosh; GraphPad Inc., San Diego, California, USA). A *P* value of less than .05 was considered significant.

RESULTS

Patient characteristics

Clinical characteristics of all patients are summarized in Table E1 (available in this article's Online Repository at www.jaci-inpractice.org). The 21 individuals were from 17 unrelated families. There were 12 males and 9 females. At the time of inclusion, 3 patients had died (at the ages of 29 years [P2], 34 years [P6], and 11 years [P11]). Living patients had a median age of 8 years (0.6-65 years) at the time of censoring of data collection.

Molecular data

The 21 patients of our cohort carried the p.V155M (n = 13), p.N154S (n = 4), p.V147M (n = 1), p.C206Y (n = 1), or p.R281Q (n = 2) substitutions in STING (Figure 1, *A*, and Table E2, available in this article's Online Repository at www.jaci-inpractice.org). All these substitutions have been previously shown to result in STING gain-of-function. In 12 patients, the mutation occurred *de novo*, whereas in 4 patients from 2 unrelated families, dominant inheritance was confirmed (see Table E2 in this article's Online Repository at www.jaci-inpractice.org). In 5 cases, inheritance could not be determined (no available DNA from both parents). Genetic diagnosis was made at a median age of 8.5 years (1.25-65 years) and retrospectively in P2, P6, and P11.

Clinical phenotype

The median age of disease onset was 8.5 months (birth to 13 years) with most patients being symptomatic by the age of 1 year (14 of 20, 70%) (Table I and Figure 1, *B*). Onset of the disease in P4 could not be assessed with accuracy, but was in adulthood. Initial diagnoses before genetic testing are given in Figure 1, *C*. Of note, P2 and P3 received a first diagnosis of polyarthritis and P16 of combined immunodeficiency (CID), representing 2 original clinical presentations.

Failure to thrive was a common feature, with weight and height being below −2 standard deviations (SD) in, respectively, 15 of 20 and 10 of 20 patients. A severe growth failure with height <−3 SD was striking in 4 patients observed independently of steroid exposure. The frequency of the various features is given in Figure 1, *D*. A comparison with patients reported in the literature is provided in Table I.

Skin disease

Eighteen patients (86%) displayed skin disease of variable severity, whereas 3 patients (P4, P12, and P16 at the ages of 65, 12, and 0.7 years, respectively) have never demonstrated cutaneous involvement (Figures 1, *D*, and 2). Six patients (29%) exhibited severe skin vasculopathy, predominantly involving the nose, cheeks, ears, fingers, and toes, and 4 patients (19%) presented extreme skin phenotype with extensive tissue loss. Milder lesions occurred in 8 individuals (38%), comprising acral and malar rash, mild cold-induced ulcers, telangiectasia, and livedo. Perforation of the nasal septum was recorded in 3 patients. When performed (n = 6), capillaroscopy was uninformative (normal in 5 cases of mild or severe cutaneous involvement, and showing a nonspecific microangiopathy in 1 case of extreme skin vasculopathy). Nail dystrophy was seen in 7 patients, whereas alopecia was noted in 2 patients, and sparse and thin hair in 5. Oral mucosal lesions (gingivostomatitis, aphtosis) occurred in 4 patients.

Lung phenotype

Pulmonary disease was noted in all patients and was associated with a high degree of disability and mortality, although heterogeneity was observed across the cohort (Figure 3, *A*). Onset occurred early in the course of the disease—in infancy or early childhood—although the involvement was diagnosed after lung investigations in 3 patients (P4, P13, and P15) with few respiratory symptoms at 64, 17, and 6 years, respectively. Symptoms were initially insidious, characterized by early-onset progressive dyspnea (n = 16), and/or tachypnoea (n = 11), and/or cough (n = 7). Nine patients required supplemental oxygen therapy at onset (n = 7, transiently in P16) or during the course of the disease (n = 8), of whom 6 progressed to end-stage respiratory failure in adolescence or early adulthood, necessitating noninvasive ventilation in 4 cases. One patient (P6) underwent lung transplantation, and 2 others (P7 and P12) were programmed for lung transplantation. Hypoxia-related pulmonary hypertension was documented in 2 patients.

A first assessment of pulmonary function was made in 15 patients at diagnosis and during the course of disease, at a median age of 8.7 years (3.08-27 years) (see Table E3 in this article's Online Repository at www.jaci-inpractice.org). Lung volumes were initially normal in 2 patients. The other patients displayed a restrictive (n = 11) and/or hyperinflation pattern (n = 9). Two patients also demonstrated features of pulmonary obstruction.

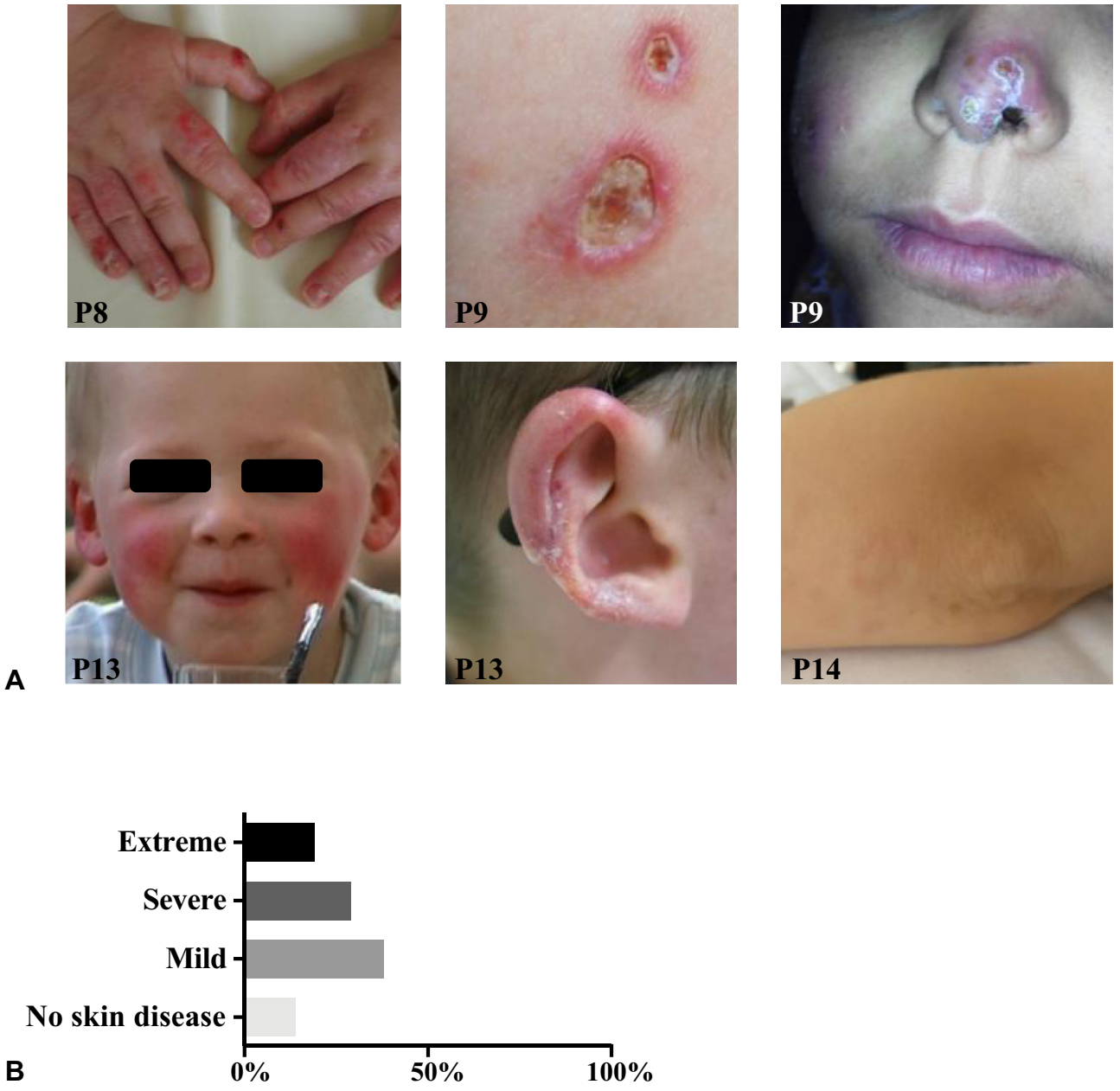

FIGURE 2. Cutaneous involvement observed in the patients. **A**, Representative cutaneous involvement observed in 4 patients of the cohort, demonstrating erythematous infiltrated plaques with ulcerations on the dorsal side of the fingers and mild nail dystrophy (P8), round-like ulcerations on the dorsal side of the right leg and ulceration of the nose and the right cheek (P9), facial erythema and telangiectatic lesions of the cheeks and erythema and ulceration of the outer helix of the right ear (P13), and urticarial-like lesions of the right elbow (P14). **B**, Severity distribution of the skin disease, classified as absent, mild, severe, or extreme. The latter included perforation of the nasal septum and lesions leading to digital amputation and other tissue loss.

Diffusing capacity of the lungs for carbon monoxide with values below 80% of the predicted values was recorded in 9 of 11 patients evaluated for this parameter. Among 6 patients who had a 6-minute walking test, the walking distance was reduced in 5, and associated with a fall in oxygen saturation. When repeated during the course of the disease, functional parameters worsened or became impaired in all patients assessed (n = 15) (see Table E3 in this article's Online Repository at www.jaci-inpractice.org).

Chest CT scans were reviewed in 16 patients. A summary of the analysis of the first thoracic imaging available for each patient (performed at a median age of 6 years [0.6-65 years]) is provided in Table E4 (available in this article's Online Repository at www.jaci-inpractice.org). Key elementary lesions observed in the majority of patients were ground-glass opacities (n = 13) with crazy paving pattern (n = 11) and cysts (n = 10) (either microcysts [n = 8] and/or macrocysts [n = 4]) (Figure 3, *B-F*). Of particular interest, in contrast to those described in ILD associated with

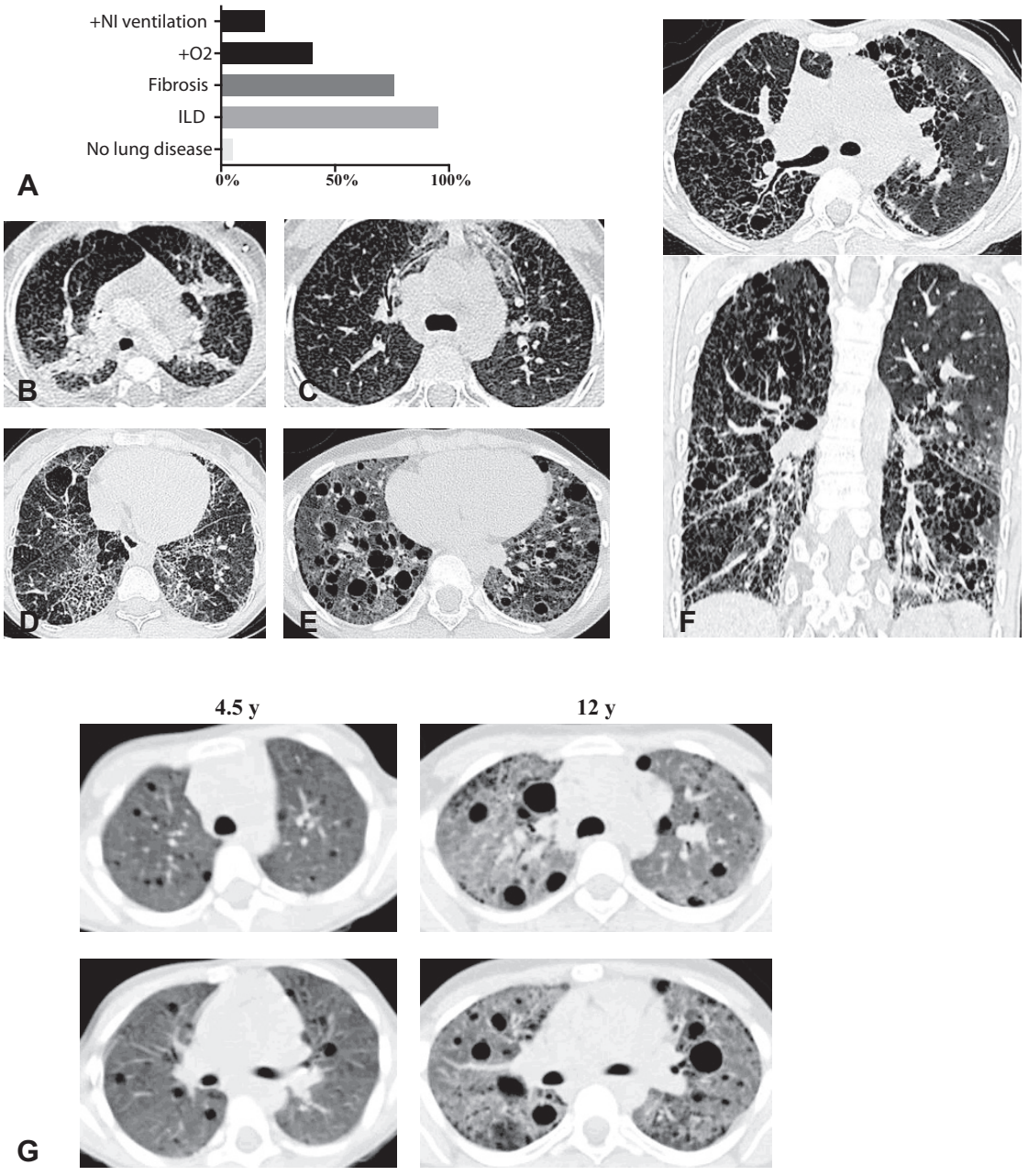

FIGURE 3. Lung involvement observed in the patients. **A**, Severity distribution of pulmonary disease, classified as interstitial lung disease (ILD), fibrosis, requirement for oxygen therapy ($+O_2$), and requirement for noninvasive ventilation (+NI ventilation). **B**-**F**, Key elementary radiological features observed in the patients. **B**, P16 at 6 months old. Retractile areas of ground-glass opacities, with a random and asymmetrical disposition, diffuse thickened intralobular lines in the periphery of the lung. The presence of distension in the anterior parts of the lung. **C**, P14, aged 7 years and 10 months. The presence of ground glass opacities located in the anterosuperior zones of the lung, associated with traction bronchiectasis. Diffuse thickened intralobular lines are present in the subpleural zones of the lung. **D**, P21, 23 years old. Asymmetrical interstitial lung involvement predominant in the right lung and left lower lobe. Ground-glass opacities, coarse thickening of the intralobular lines associated with microcystic honeycombing. Emphysematous area lobules are also present. **E**, P12, aged 12 years: diffuse ground-glass opacities associated with a thickening of the intralobular lines and subpleural microcystic lesions. Scattered macrocystic lesions are also present, some of which contain a central arteriole, suggesting lesions of central-lobular emphysema despite the presence of thick walls. **F**, P7, aged 13 years and 10 months. Almost complete destruction of the right lung and the left lower lobe by lesions of macrocystic honeycombing. Diffuse ground-glass opacities are seen in the areas of the left lung spared from the fibrosis. **G**, Chest computed tomography scan of P12 performed at the age of 4.5 years (left panels) demonstrated diffuse ground-glass lesions and interlobular septal thickening, subpleural intralobular lines, and cysts predominantly located in the lower lobes. At the age of 12 years (right panels), the intensity of the ground-glass lesions has increased, as well as the number and size of the cystic lesions, with evidence of macrocysts and subpleural microcysts. The latter, constituting honeycombing and traction bronchiectasis, were indicative of fibrotic progression.

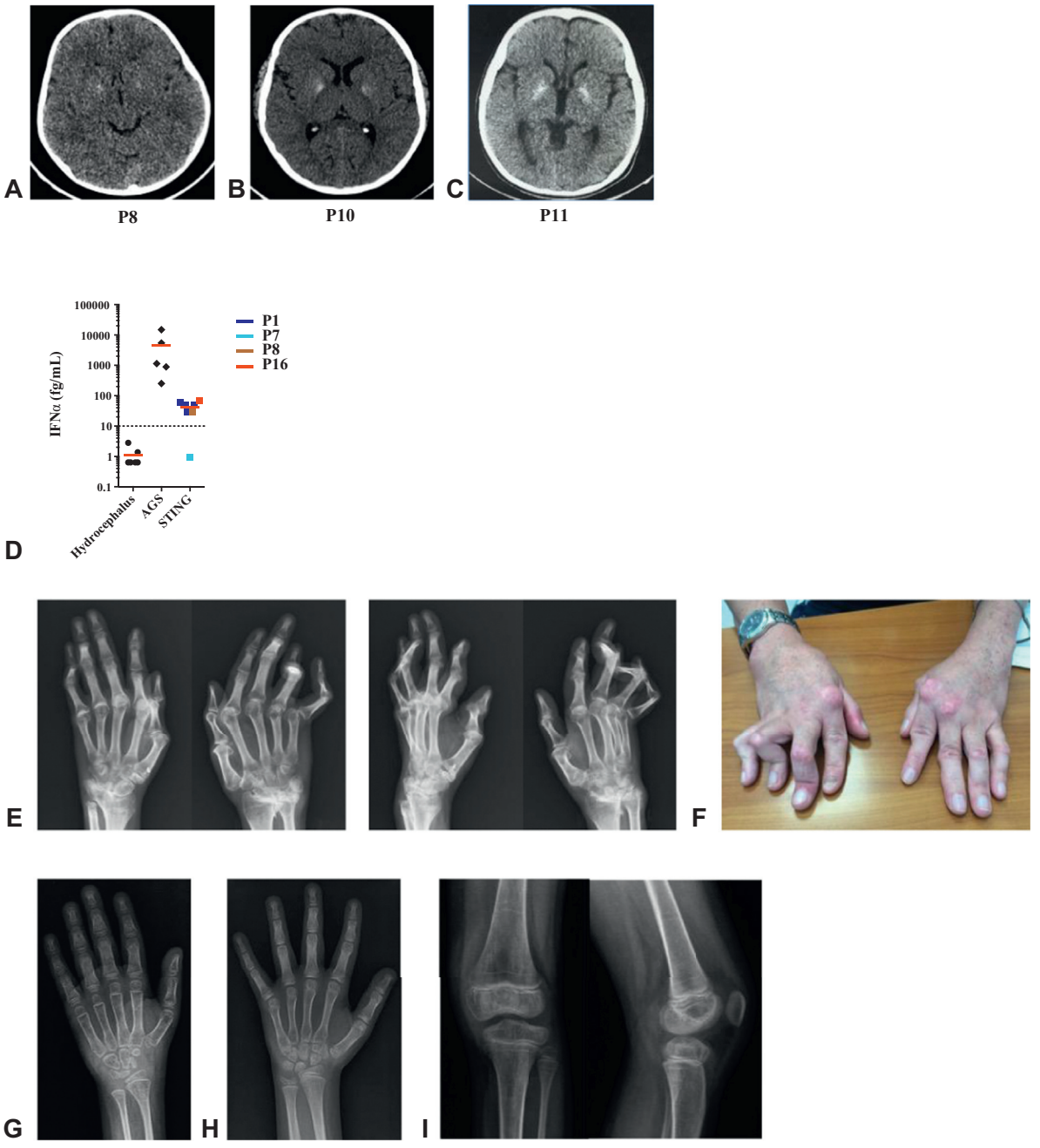

FIGURE 4. Intracranial calcifications, levels of interferon alpha protein in the cerebrospinal fluid observed in the cohort, and joint involvement observed in the patients. **A**-**C**, Brain computed tomography scan demonstrating calcifications of the globi pallidi in P8 (**A**, at the age of 8 years), P10 (**B**, at the age of 15 years), and P11 (**C**, at the age of 9 years). **D**, Levels of interferon alpha protein (IFNα) measured by ultrasensitive digital ELISA[25] (normal <2 fg/mL) in the cerebrospinal fluid of 4 patients of the cohort (n = 7 samples), 5 patients with Aicardi-Goutières syndrome (AGS) (n = 5 samples), and 6 children with noninflammatory idiopathic hydrocephalus as controls (n = 6 samples). **E**, Conventional anteroposterior and lateral X-rays of the hands of P3 performed at the age of 33 years demonstrating subluxation of metacarpophalangeal and interphalangeal joints, predominantly on the right side. No erosions were observed. **F**, Hand deformities present in P3 at the age of 36 years, including boutonnière and swan neck deformities. These aspects are reminiscent of Jaccoud's arthropathy,[31,32] a phenotype present mostly in patients with systemic erythematosus lupus where hand deformities are passively correctable and not associated with bone erosions on X-ray. **G**,**H**, Conventional anteroposterior X-rays of the left hand of P14 performed at the age of (**G**) 5 and (**H**) 10 years demonstrating delayed bone age and bone demineralization with joint space narrowing and erosions on carpal bones. No luxation of metacarpophalangeal or interphalangeal joints was observed. **I**, Conventional anteroposterior and lateral X-rays of the left knee in P14 performed at the age of 8 years, showing bone demineralization. *STING*, Stimulator of Interferon Genes.

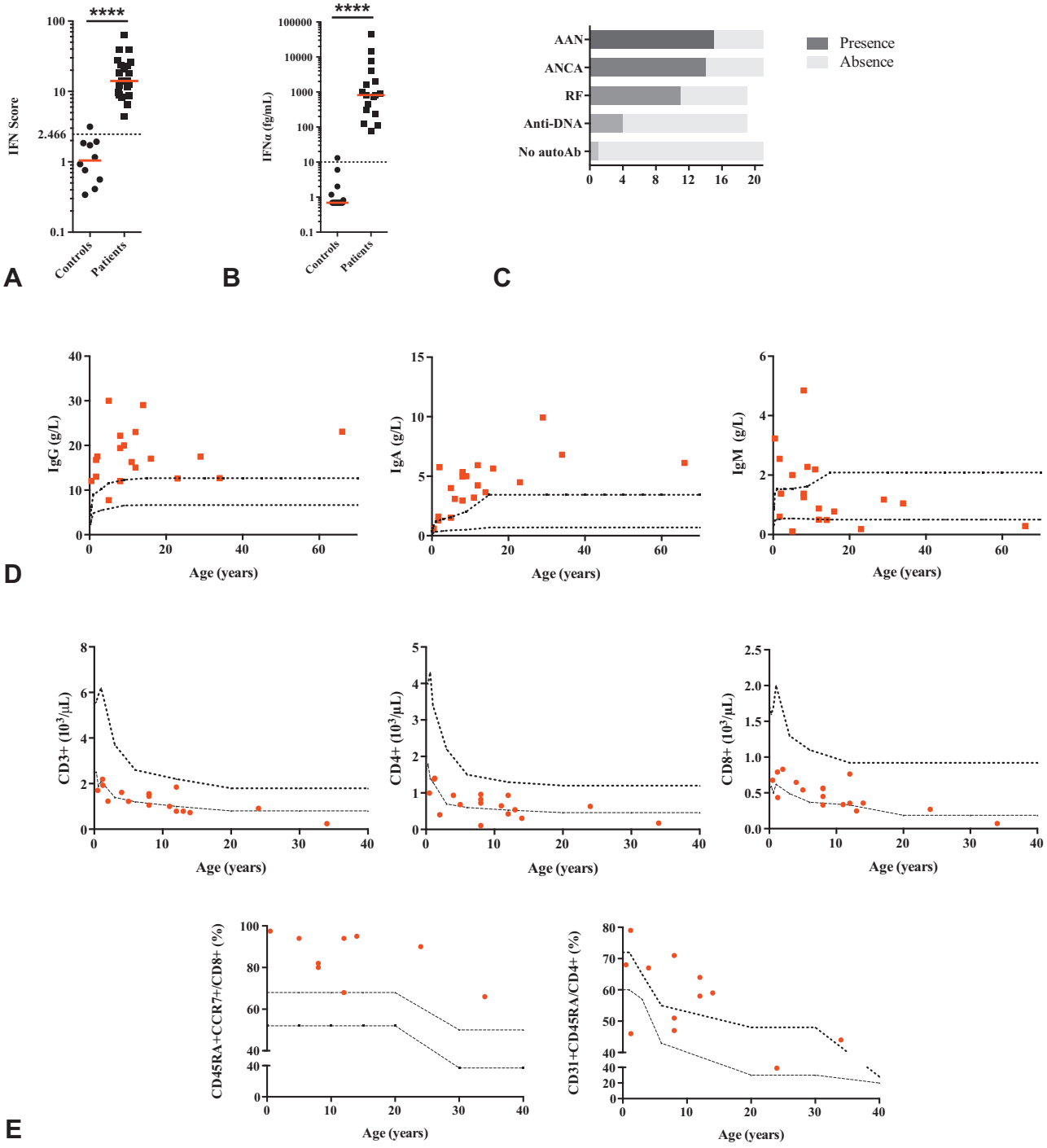

FIGURE 5. Immunological features of the patients. **A**, IFN scores calculated from the median fold change in relative quantification values for the set of 6 ISGs[28] (*IFI27*, *IFI44L*, *IFIT1*, *ISG15*, *RSAD2*, *SIGLEC1*, normal <2.466) recorded in patients, as compared with 10 healthy controls (n = 10). The median value in patients (14.08; interquartile range [IQR], 9.417-24.72) was significantly higher than that in healthy controls (1.045; IQR, 0.5225-1.870); ****$P < .0001$ using the Mann-Whitney test. **B**, Concentrations of IFNα protein (healthy controls <10 fg/mL) assessed by ultrasensitive digital ELISA[25] in plasma or serum from healthy controls (n = 20) and 9 patients of the cohort (n = 17 samples in total). The median value in patients (817.8 fg/mL; IQR, 274.8-3039) was significantly higher than that in healthy controls (0.69 fg/mL; IQR, 0.69-0.78); ****$P < .0001$ using the Mann-Whitney test. **C**, Autoantibodies observed in the cohort: antinuclear antibodies (ANA), antineutrophil cytoplasm antibodies (ANCA), rheumatoid factor (RF), anti–double stranded DNA (anti-DNA). The presence of an autoantibody is depicted in dark gray and its absence in pale gray, thus indicating the number of patients assessed. One patient of the cohort had no autoantibodies ("no autoAb"). **D**, Levels of IgG, IgA, and IgM. The dotted lines indicate the minimum and maximum ranges according to age. **E**, Numbers of CD3+, CD4+, and CD8+ lymphocytes and percentage (%) of CD4+ naïve T cells (CD31+CD45RA+/CD4+ cells) and CD8+ naïve T cells (CD45RA+CCR7+/CD8+ cells). The dotted lines indicate the reference ranges for immunophenotyping data according to age.[33]

TABLE II. Treatment with ruxolitinib in the cohort

	Age at initiation (y)	Follow-up (mo)	Initial dosing (mg/kg/d)	Dosing at last follow-up (mg/kg/d)	Concomitant treatments at JAKi initiation	IVIg	Time to discontinuation of steroids (mo)	Time to discontinuation of DMARDs (mo)	Time to discontinuation of biologics (mo)	Infectious adverse effects	Other adverse side effects
P1	4	52 (switch tofacitinib)	0.48	1	Steroids (0.5)	Yes	9	–	–	No	Papillary edema[26] Rebound effect
P5	12	30 (switch baricitinib)	0.38	0.45	Steroids (0.2) HCQ	No	1	No (still on HCQ)	–	Zona, BK viremia (nonquantifiable)	Rebound effect
P7	14.2	2.5 (transplant)	0.32	0.28	Steroids (0.16)	No	Steroids (0.16 each 2 days)	–	–	Rhinovirus	No
P8	8.4	50	0.26	1.11	Steroids (0.6)	No	8	–	–	Zona, cutaneous infection (*Staphylococcus aureus*)	No
P9	7.8	41	0.31	1.10	Steroids (0.625)	Yes	29 (pulse of steroids at M37 for arthritis)	–	–	H1N1 influenza Upper respiratory tract infections (4 episodes, no identified organism)	No
P12	12.5	17 (transplant)	0.2	0.2	Steroids (1.5) and monthly steroid pulse	Yes	7 (stop pulses at initiation of JAKi)	0 (MMF)	–	Pneumonia (no identified organism) Aspergilloma (diagnosed by histological analysis of her native lung)	No
P14	8	18	0.44	0.83	Steroids (0.22) Monthly steroid pulse Etanercept	No	3	–	No (decrease of dosing of etanercept)	No	No
P16	0.6	24	0.83	1	–	Yes	–	–	–	No	No

DMARD, Disease-modifying antirheumatic drug; *HCQ*, hydroxychloroquine; *IVIg*, intravenous immunoglobulins; *JAKi*, JAK inhibitor; *MMF*, mycophenolate mofetil; *mo*, month; *y,* year.

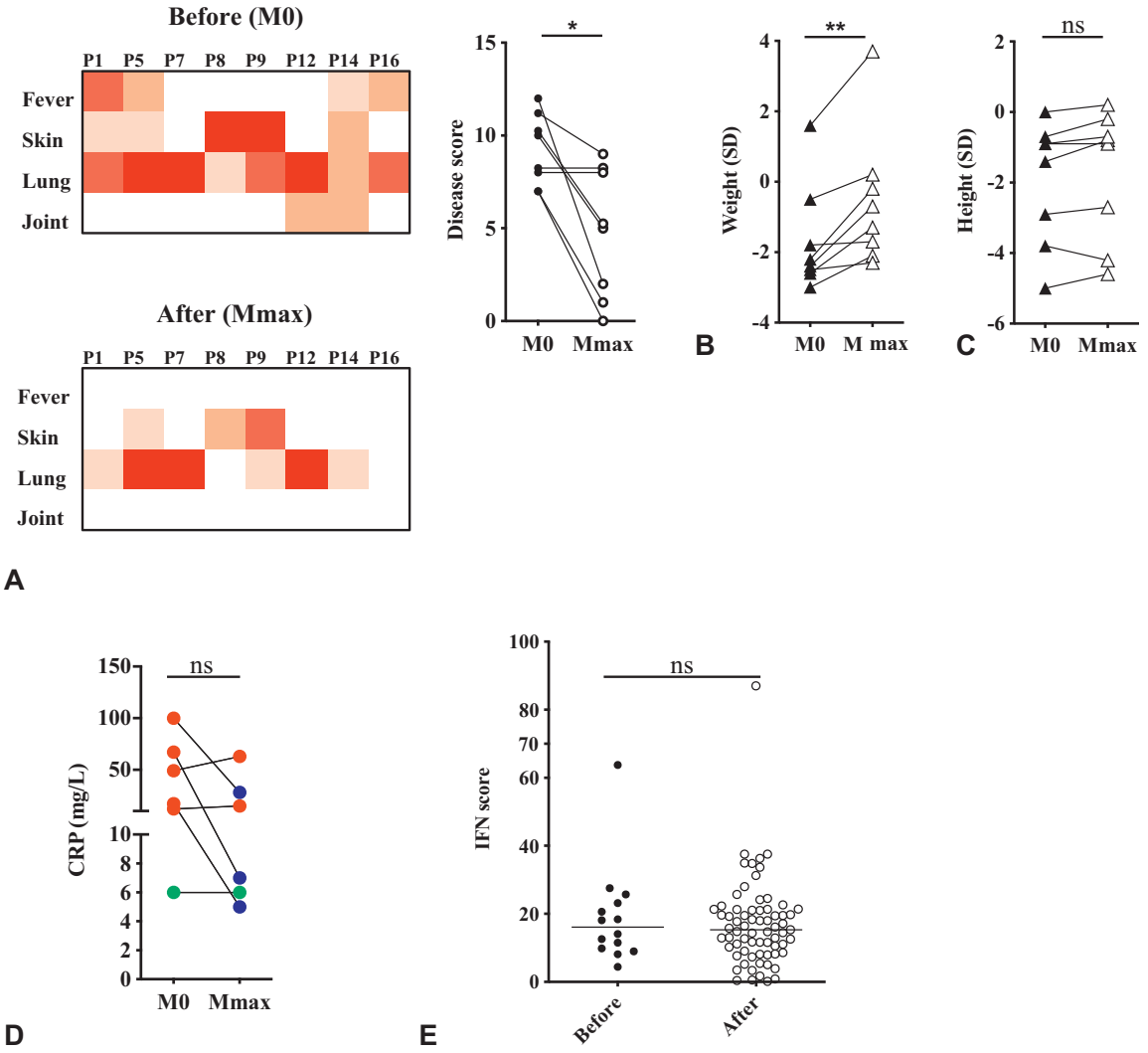

FIGURE 6. Response to ruxolitinib in the cohort. **A**, Left panel: schematic representation of the clinical response of the patients to ruxolitinib. Upper panel: last clinical status before ruxolitinib (M0); lower panel: clinical status at maximal follow-up available (Mmax) (for P7 and P12, the last follow-up recorded was before their lung transplantation). "Fever," "Skin," and "Lung" items were represented according to the patients' disease scores (see the right panel). In brief, Fever: white, no fever; beige, fever every month; salmon, fever every week; red, fever twice a week; dark red, fever every day. Skin: white, absence of cutaneous lesions; beige, mild vasculopathy; salmon, severe vasculopathy; red, extreme vasculopathy; dark red, presence of extensive tissue loss or nasal perforation. Lung: white, no dyspnea; beige, dyspnea on intense exercise, rapid breathing, but with no functional impact; salmon, dyspnea on moderate exercise, rapid breathing, with mild functional impact; red, severe dyspnea at rest, rapid breathing, occurring with severe functional impact (eg, absence from school or work); dark red, severe dyspnea at rest, rapid breathing, resulting in staying in bed, oxygen therapy. "Joint" feature was pictured as follows: white, absence of joint disease; beige, mono- or oligoarthritis; salmon, mild polyarthritis; red, severe polyarthritis; dark red, presence of articular destruction. Right panel: disease score[26] before ruxolitinib (M0) and at maximal follow-up (Mmax). Disease scores significantly decreased under treatment (*$P < .05$ using the Wilcoxon test). **B**, Weight in standard deviation (SD) at screening (M0) and during follow-up (Mmax), demonstrating improved growth in all patients. Median weight SD improved from −2.30 (interquartile range [IQR], −2.57 to −0.82) to −1.00 (IQR, −2.00 to 0.10, **$P < .01$ using the Wilcoxon test). **C**, Height in SD at screening (M0) and during follow-up (Mmax), showing stabilized growth with no "catch-up" in 7 individuals and further growth failure in 1 patient (P1). Median height SD improved from −1.15 (IQR, −3.57 to −0.75) to −0.85 (IQR, −3.82 to −0.32, ns using the Wilcoxon test). **D**, C-reactive protein (CRP) levels (normal <6 mg/L) recorded in 6 patients at screening (M0) and at maximal follow-up (Mmax). Normal levels of CRP before treatment are depicted in green. A reduction of at least 20% in the values of CRP of Mmax as compared with M0 is represented in blue. Raised levels of CPR before treatment or decreased less than 20% at Mmax are pictured in red. Median value of CRP decreased from 33.05 mg/L (IQR, 10.5-75.25 mg/L) at M0 to 11 mg/L (IQR, 5.750-36.75 mg/L) at Mmax (nonsignificant, using the Wilcoxon test). **E**, IFN scores (normal <2.466) recorded before and during therapy. Before = recorded values before the initiation of ruxolitinib including day 0 (n = 14); After = recorded values under ruxolitinib (n = 69). Black lines represent median values by time period. Median values before and under treatment were comparable (using the Mann-Whitney test).

connective tissue disease,[29] lesions were frequently asymmetrical. Radiologically defined fibrosis was described in 12 of 16 patients as early as age 0.6 years. Serial chest CT scans were analyzed in 6 patients, further emphasizing the occurrence of severe fibrotic lesions before adulthood (see Figure 3, *G*, and Table E5, available in this article's Online Repository at www.jaci-inpractice.org).

Bronchoalveolar lavage (BAL) fluid analysis was performed in 14 patients (see Table E6 in this article's Online Repository at www.jaci-inpractice.org), with a median cellularity of 1000 (190-3400) cells/mm^3. One individual had a normal total cellularity but with an abnormal cell distribution. In the other patients, BAL fluid analysis displayed a mixed (n = 5), neutrophilic (n = 3), or lymphocytic (n = 2) alveolitis. The 2 last patients were diagnosed with probable aspergillosis and alveolar hemorrhage, respectively.

Infections

Five patients experienced significant infections. Cutaneous or osteoarticular *Staphylococcus aureus* infection occurred in 4 patients with severe skin vasculopathy. P2, who received multiple lines of immunosuppressive therapies (Table E1, available in this article's Online Repository at www.jaci-inpractice.org), experienced recurrence of herpes zoster and severe invasive or opportunistic infections (ie, necrotizing fasciitis due to *Streptococcus pyogenes*, osteitis due to *S. aureus*, and invasive pulmonary aspergillosis). Two patients with severe lung lesions (P18 and P20) had *Pseudomonas aeruginosa* colonization of the respiratory tract. No other increased susceptibility to infections was noticed in the cohort.

Neurological involvement

Neurological manifestations are not a core feature of SAVI in comparison with other monogenic interferonopathies,[4] in particular Aicardi-Goutières syndrome (AGS).[30] None of the patients presented developmental delay. However, calcification of the basal ganglia was observed in 3 of 12 patients explored with brain CT scan (Figure 4, *A-C*). Among these 3 patients, P8 was neurologically asymptomatic, P10 demonstrated a spastic diplegia, and P11 presented 2 episodes of seizure. Cerebral magnetic resonance imaging performed in 8 patients was normal in all of them. Of 8 cerebrospinal fluid (CSF) samples analyzed, 6 were normal and 2 revealed lymphocytic meningitis without evidence of infection (P2 and P3). Of interest, P12 suffered from glaucoma, as observed in AGS.[30]

Articular features

Articular manifestations were frequent (arthralgia, n = 9; arthritis, n = 7). In particular, 7 patients had polyarthritis diagnosed at a median age of 6.8 years (0.17-13 years) and that became destructive over time in P2 and P3 (Figure 4, *E* and *F*; see Figure E1 in this article's Online Repository at www.jaci-inpractice.org), necessitating a left knee prosthesis at the age of 34 years in P3. Hand and skeletal X-rays were reviewed in 9 patients, and axial osteoarticular structures were studied based on the chest CT scans in 12 patients. Delayed bone age was observed in 6 of 8 patients (Figure 4, *G* and *H*). Bone demineralization was a common feature (Figure 4, *G-I*). Condensations were seen in the peripheral skeleton (see Figure E1, *B*, in this article's Online Repository at www.jaci-inpractice.org), whereas few or no erosions or deaxation were observed (except in P3). One patient had diffuse erosions of the carpal bones reminiscent of juvenile idiopathic arthritis (JIA) (Figure 4, *G* and *H*). All polyarthritis but one were associated with rheumatoid factor (RF) positivity.

Other features

A transient episode of myositis occurred in P9, at the age of 6 years, while he was being treated with tocilizumab (an anti-IL6 receptor monoclonal antibody). All symptoms resolved after the drug was stopped. P18, previously reported in the first description of *STING1* mutations in a second mutational cluster,[10] developed evidence of hepatitis. A liver biopsy performed at age 2 years revealed granulomatous inflammation with necrosis and pericentral atrophy. We also noted cardiac disease (cardiomegaly with repolarization defects) complicated, at the age of 11 years, by subepicardial ischemia in one patient (P11), and 3 episodes of pericarditis in another patient (P12). Finally, kidney involvement was recorded in 2 patients; P17 presenting with microscopic hematuria and mild proteinuria associated with hypertension. No kidney biopsy was performed. In addition, P21 demonstrated proteinuria from the age of 3 years, associated with positive antineutrophil cytoplasmic antibodies (ANCA) and segmental glomerular and focal proliferative lesions. A kidney biopsy at the age of 10 years revealed chronic glomerular and tubule-interstitial lesions with interstitial fibrosis and progression to tubular atrophy.

Inflammatory markers

Increased levels of C-reactive protein and/or of erythrocyte sedimentation rate were observed in all but one patient (P8) (see Figure E2 in this article's Online Repository at www.jaci-inpractice.org).

Type I IFN pathway activation in patients

IFN score and IFNα protein[25] were consistently high in all patients tested (Figure 5, *A* and *B*). Of interest, we measured IFNα protein in the CSF of 4 patients with no neurological symptoms (P1, P7, P8, and P16)—of whom 1 had intracranial calcification (ICC) of the globi pallidi (P8)—and found high level although lower concentrations than in patients with AGS (manuscript in preparation). However, these levels were higher in 3 patients of the cohort than in children with idiopathic hydrocephalus (Figure 4, *D*). As previously reported,[1,26,27] increased levels of STAT1 phosphorylation were recorded in T lymphocytes, monocytes, and neutrophils of 7 patients explored (data not shown).

Autoantibodies

All patients but one (P13) presented autoantibodies. High titers of antinuclear antibodies (15 of 21) and ANCA with low specificity for MPO and PR3 (15 of 21) were seen frequently (Table E1, available in this article's Online Repository at www.jaci-inpractice.org, and Figure 5, *C*). Increased RF was documented in 11 of 18 patients. All patients but one presented hyper-IgG and -IgA, whereas IgM levels were variable (Figure 5, *D*). Complement levels were normal in all patients tested (n = 15).

Immunophenotyping analyses

Mild CD3+ and CD4+ T-cell lymphopenia was frequent, documented in 10 of 17 (59%) and 6 of 17 (35%) patients,

respectively. Decreased percentage of central memory CD8+ (CCR7+CD45RA−/CD8+) (n = 7 of 9, 78%) and effector memory CD8+ (CCR7−CD45RA−/CD8+) (n = 8 of 9, 89%) T cells with increased percentage of naïve CD4+ (n = 7 of 12, 58%) and CD8+ (n = 8 of 9, 89%) T cells were frequently observed (Figure 5, *E*). T-cell proliferation in response to mitogens was normal in most patients tested (n = 12 of 15), but frequently impaired in response to antigens (n = 5 of 6) or OKT3 (n = 6 of 8). Extended B-cell phenotyping revealed low memory B-cell counts (CD19+CD27+) in 9 of 10 patients (data not shown).

Treatment and clinical outcome

Three patients were deceased, including 1 patient who succumbed early after lung transplantation (P6) and 1 due to end-stage respiratory failure (P11). The third patient (P3) died at the age of 29 years of fulminant necrotizing fasciitis. All patients but 3 received steroids and 12 were treated with several lines of immunosuppressive therapy, including methotrexate, mycophenolate mofetil, and biologics (Table E1, available in this article's Online Repository at www.jaci-inpractice.org). There was apparently no, or little, response to these treatments.

Experience with JAK inhibitors in the cohort

Subsequently after the end point of this overview, 17 patients were treated with JAK inhibitors, allowing rapid clearance of fever, heterogeneous improvement of lung, and skin diseases depending on severity and damage. We report here the extensive assessment of response to JAK inhibition in 8 pediatric patients treated in France, at a median age of 8.2 years (0.6-14.2 years) at drug initiation (Table II). Main involvements were the lung (n = 8, all with fibrosis but one, including 3 patients with end-stage respiratory failure screened for lung transplantation) and skin (n = 5, including 2 with extreme lesions), whereas 2 patients suffered from polyarthritis. The median initial dose of ruxolitinib was 0.32 (0.2-0.83) mg/kg/day bid, which was increased to 0.9 (0.2-1.11) mg/kg/day bid based on pharmacokinetic studies. The median follow-up under treatment was 27 (2.5-52) months. Two patients experienced withdrawal syndrome after a short interruption of treatment.[26] Papillary edema was observed in P1.[26] Infections were reported in 5 patients (Table II), in particular a rhinovirus infection in P7 that precipitated respiratory failure and lung transplantation. In addition, aspergilloma was found in the explanted lungs of P12 at the time of transplantation. None of the patients developed anemia or thrombocytopenia. Disease score significantly improved in all patients (Figure 6, *A*). Fever settled in all patients, and skin manifestations resolved in 2 patients and improved in 2. Among the 3 patients with severe lung involvement, P5 experienced clinical benefice, and P7 and P12 had a minimal improvement and were transplanted 3 and 17 months, respectively, after ruxolitinib initiation. P7 died of humoral rejection 1 year later, whereas P12 is alive and well 2 years after transplantation under ruxolitinib. In 5 patients, pulmonary functional and radiological improvements were significant (Figure 6, *A*, and Table E7 and Figure E3, *A* and *B*, available in this article's Online Repository at www.jaci-inpractice.org). Polyarthritis completely resolved in 2 affected patients. All patients gained weight but catch-up growth was not significant (Figure 6, *B* and *C*). There was a reduction of inflammatory markers, whereas median IFN scores across patients were comparable (Figure 6, *D* and *E*, and Figure E3, *C*, available in this article's Online Repository at www.jaci-inpractice.org). Immunophenotyping and autoantibodies remained stable.

DISCUSSION

Activating mutations in *STING1* were described in 2014 to cause a novel type I interferonopathy, referred to as SAVI.[1,2] This severe autoinflammatory condition was minimally responsive to conventional immunosuppressive therapies, and thus was associated with marked childhood morbidity and increased mortality.[1,2,5-24]

The present cohort of 21 patients (17 families) confirms the severity of SAVI and high incidence of the core features, that is, skin and lung involvement and systemic inflammation. As reported in the literature (Table I), early disease onset was the rule, except for P4 who displayed adulthood onset and suffered from a milder disease. Although phenotypic differences have been suggested between mutations occurring in exon 5 and exons 6 and 7,[13,15] this is not obviously the case in our cohort, that is, we are unable to define a genotype-phenotype correlation with the data available so far.

Lung involvement was the most striking feature observed in all patients (vs 68% of the reported cases). Respiratory symptoms may be insidious, with infraclinic involvement identified after radiologic and functional investigations. This advocates for systematic lung screening in patients with suspected or confirmed SAVI. ILD and fibrosis can be isolated as previously reported,[7] and SAVI should be considered in front of idiopathic lung fibrosis occurring in children or young adults, particularly in the presence of autoantibodies or immunological abnormalities such as memory CD8 lymphopenia. The radiological hallmark of the pulmonary syndrome in the present cohort was an early and rapid progression to fibrosis—distinct from the usual imaging findings seen in chronic ILD in children[34,35]—observed in 76% of patients (vs 25% in the literature). We confirmed the high lung-related morbidity and mortality, with end-stage respiratory failure in 6 patients by early adulthood. Moreover, lung transplantation was performed in 1 young adult patient who died early thereafter, and in 2 teenage patients after censoring of the data. The outcome of these patients could not help to evaluate the risk of relapse on transplanted lungs. Although type I IFN is suggested to contribute to the lung fibrosis occurring in systemic sclerosis,[36,37] the pathogenesis of interstitial lesions and fibrotic progression in SAVI remains to be deciphered. STING gain-of-function knock-in mice[38-41] develop alveolar infiltration, and also perivascular inflammation—a feature that has not been reported so far in humans with SAVI. Of note, the pulmonary pathology of the STING N153S or V154M mutant mice was not rescued by crossing onto an *Irf3* or *Ifnar1* null background,[38,40,41] thereby suggesting the complexity of lung pathogenesis in SAVI. However, STING gain-of-function mice models so far developed do not fully recapitulate the phenotype in humans, further emphasizing the need of patient cohorts to study the spectrum and underlying mechanisms of SAVI.

Our cohort further extends the clinical phenotype of SAVI, including features reminiscent of other monogenic interferonopathies.[4,42] A distinctive osteoarticular involvement was

found in 1 one third of the cohort. Indeed, polyarticular RF+ JIA was the initial diagnosis in 3 patients (as reported by Clarke et al[21]), among whom long-term evolution has been characterized by marked articular damage in 2 individuals. Of interest, positivity for RF was recorded in 11 of 19 patients tested (58%). This suggests that RF could be a useful diagnostic marker of SAVI, especially in childhood, during which polyarticular RF+ JIA rarely occurs.[43] Cardiac involvement has not been previously reported in the context of SAVI and is not a common feature in other monogenic interferonopathies, beyond infantile-onset hypertrophic cardiomyopathy described in 3.3% of patients with AGS.[30] Three individuals in this report demonstrated ICC of the basal ganglia, a well-known imaging characteristic of AGS.[44] Spastic diplegia was marked in one of them, thereby indicating a possible overlap between SAVI and AGS, in which a severe skin vasculopathy can also be observed.[4,30] Of note, 1 patient with ICC was neurologically asymptomatic, as can be observed in certain neurological diseases including the type I interferonopathy due to ISG15 loss-of-function,[45] but the possibility remains that neurological dysfunction is more frequent than currently appreciated and may become evident over time. Of interest, 1 patient presented with alveolar hemorrhage during the course of the disease. Although reported in only 1 SAVI individual,[19] alveolar hemorrhage is a striking feature of COPA (coatomer protein subunit α) syndrome,[46] a newly described interferonopathy physio-pathologically related to SAVI.[47-49] Renal glomerular disease was noticed in our cohort. Such involvement is also reported in other monogenic interferonopathies (DNaseII deficiency,[50] COPA[46,51]).

Our cohort reveals a specific immunological pattern in the context of SAVI, defined by low counts of CD4+ and CD8+ T cells, and high percentage of naïve CD4+ and CD8+ T cells associated with a defect in circulating memory CD4+ and CD8+ T cells. A partial defect in T-cell proliferation was also frequently noticed. Despite these features, the patients in our cohort did not display opportunistic infection. One can hypothesize that the enhanced type I IFN production observed in SAVI partially compensates cellular immune defect. This point highlights the potential risk of infection with the use of JAK inhibitors, which block several cytokine pathways. Of interest, a patient with SAVI, presenting at age 2 months with *Pneumocystis jirovecii* pneumonia and severe T-cell lymphopenia, has been reported.[15] We also described 1 child with initial diagnosis of CID. These observations highlight the variable onset and expression of SAVI, and are reminiscent of the mild to extremely severe lymphopenia recorded in the published STING gain-of-function mouse models (N153S and V154M).[38-41] Of further note, the defect in T-cell proliferation demonstrated by patients with SAVI is consistent with the report of Cerboni et al[52] where the authors showed an intrinsic antiproliferative action of activated STING in patient and mouse cells. More recently, further IFN-independent functions of STING have been established.[53,54]

Long-term follow-up of 8 patients under ruxolitinib confirms improvement of all SAVI features in line with the experience reported in the literature.[16,27] The best response was observed in patients treated early before the occurrence of irreversible damage especially to the lung, underlying the importance of early diagnosis. Tolerance was overall good, but the risk of viral respiratory infections in patients with poor lung function deserves particular attention.[16] Of note, Sanchez et al[27] reported a BK viremia in half of the patients with interferonopathies treated with baricitinib, a complication seen in only 1 patient in our cohort. As previously described,[26,27] there was no control of the enhanced ISG expression. Further pharmacokinetic studies are required to better determine dosage and timing in the use of each JAK inhibitor. Other therapeutic strategies with new-generation JAK inhibitors or STING inhibitors[55] are awaited.

Overall, we describe, to our knowledge, the largest cohort of SAVI worldwide. Together with a high penetrance of key features, we note a variability in severity, highlighted the lung-related morbidity-mortality, and a frequent joint involvement. Rare manifestations overlapping with other monogenic interferonopathies can occur, indicating—at least partially—redundant physiopathology. We recommend an assessment of IFN pathway and screening of activating mutations in *STING1* in patients with lupus chilblain, polyarticular RF+ JIA, idiopathic ILD occurring in children or young adults especially in presence of autoantibodies, and CID in particular with memory CD8 T-cell lymphopenia and antigen proliferation defect. Because of complexity of SAVI, a multidisciplinary team is required to manage these patients.

Acknowledgments

The authors wish to thank the patients and their families for their cooperation in this study. The authors are grateful to Elvira Duchesne (NP) and Samira Plassart (PhD) for their very helpful technical assistance. They thank Thomas Blauwblomme (MD, PhD, Neurosurgery Unit, Necker Hospital, Paris, France) for providing CSF from children with idiopathic hydrocephalus. M.-L. Frémond received a grant from the Institut National de la Santé et de la Recherche Médicale (reference: 000427993). Y. J. Crow acknowledges the European Research Council (GA309449 and 786142-E-T1IFNs) and a state subsidy managed by the National Research Agency (France) under the "Investments for the Future" program bearing the reference ANR-10-IAHU-01. Y. J. Crow and D. Duffy acknowledge the National Research Agency (France) (grant CE17001002).

REFERENCES

1. Liu Y, Jesus AA, Marrero B, Yang D, Ramsey SE, Sanchez GAM, et al. Activated STING in a vascular and pulmonary syndrome. N Engl J Med 2014; 371:507-18.
2. Jeremiah N, Neven B, Gentili M, Callebaut I, Maschalidi S, Stolzenberg M-C, et al. Inherited STING-activating mutation underlies a familial inflammatory syndrome with lupus-like manifestations. J Clin Invest 2014;124:5516-20.
3. Crow YJ. Type I interferonopathies: a novel set of inborn errors of immunity. Ann N Y Acad Sci 2011;1238:91-8.
4. Rodero MP, Crow YJ. Type I interferon-mediated monogenic autoinflammation: the type I interferonopathies, a conceptual overview. J Exp Med 2016;213:2527-38.
5. Munoz J, Rodière M, Jeremiah N, Rieux-Laucat F, Oojageer A, Rice GI, et al. Stimulator of interferon genes-associated vasculopathy with onset in infancy: a mimic of childhood granulomatosis with polyangiitis. JAMA Dermatol 2015; 151:872-7.
6. Omoyinmi E, Melo Gomes S, Nanthapisal S, Woo P, Standing A, Eleftheriou D, et al. Stimulator of interferon genes-associated vasculitis of infancy. Arthritis Rheumatol 2015;67:808.

7. Picard C, Thouvenin G, Kannengiesser C, Dubus J-C, Jeremiah N, Rieux-Laucat F, et al. Severe pulmonary fibrosis as the first manifestation of interferonopathy (TMEM173 mutation). Chest 2016;150:e65-71.
8. Chia J, Eroglu FK, Özen S, Orhan D, Montealegre-Sanchez G, de Jesus AA, et al. Failure to thrive, interstitial lung disease, and progressive digital necrosis with onset in infancy. J Am Acad Dermatol 2016;74:186-9.
9. Clarke SLN, Pellowe EJ, de Jesus AA, Goldbach-Mansky R, Hilliard TN, Ramanan AV. Interstitial lung disease caused by STING-associated vasculopathy with onset in infancy. Am J Respir Crit Care Med 2016;194:639-42.
10. Melki I, Rose Y, Uggenti C, Van Eyck L, Frémond M-L, Kitabayashi N, et al. Disease-associated mutations identify a novel region in human STING necessary for the control of type I interferon signaling. J Allergy Clin Immunol 2017;140:543-552.e5.
11. König N, Fiehn C, Wolf C, Schuster M, Cura Costa E, Tüngler V, et al. Familial chilblain lupus due to a gain-of-function mutation in STING. Ann Rheum Dis 2017;76:468-72.
12. Manoussakis MN, Mavragani CP, Nezos A, Zampeli E, Germenis A, Moutsopoulos HM. Type I interferonopathy in a young adult. Rheumatology 2017;56:2241-3.
13. Konno H, Chinn IK, Hong D, Orange JS, Lupski JR, Mendoza A, et al. Pro-inflammation associated with a gain-of-function mutation (R284S) in the innate immune sensor STING. Cell Rep 2018;23:1112-23.
14. Yu ZX, Zhong LQ, Song HM, Wang CY, Wang W, Li J, et al. [Stimulator of interferon genes-associated vasculopathy with onset in infancy: first case report in China]. Zhonghua Er Ke Za Zhi 2018;56:179-85.
15. Saldanha RG, Balka KR, Davidson S, Wainstein BK, Wong M, Macintosh R, et al. A mutation outside the dimerization domain causing atypical STING-associated vasculopathy with onset in infancy. Front Immunol 2018;9:1535.
16. Volpi S, Insalaco A, Caorsi R, Santori E, Messia V, Sacco O, et al. Efficacy and adverse events during janus kinase inhibitor treatment of SAVI syndrome. J Clin Immunol 2019;39:476-85.
17. Shoman W, El Chazli Y, ElSawy I, Aróstegui JI. First Egyptian patient with STING-associated vasculopathy with onset in infancy. Scand J Rheumatol 2019;48:338-9.
18. Balci S, Ekinci RMK, de Jesus AA, Goldbach-Mansky R, Yilmaz M. Baricitinib experience on STING-associated vasculopathy with onset in infancy: a representative case from Turkey. Clin Immunol 2020;212:108273.
19. Tang X, Xu H, Zhou C, Peng Y, Liu H, Liu J, et al. STING-associated vasculopathy with onset in infancy in three children with new clinical aspect and unsatisfactory therapeutic responses to tofacitinib. J Clin Immunol 2020;40:114-22.
20. Keskitalo S, Haapaniemi E, Einarsdottir E, Rajamäki K, Heikkilä H, Ilander M, et al. Novel TMEM173 mutation and the role of disease modifying alleles. Front Immunol 2019;10:2770.
21. Clarke SLN, Robertson L, Rice GI, Seabra L, Hilliard TN, Crow YJ, et al. Type 1 interferonopathy presenting as juvenile idiopathic arthritis with interstitial lung disease: report of a new phenotype. Pediatr Rheumatol Online J 2020;18:37.
22. Lin B, Berard R, Al Rasheed A, Aladba B, Kranzusch PJ, Henderlight M, et al. A novel STING1 variant causes a recessive form of STING-associated vasculopathy with onset in infancy (SAVI). J Allergy Clin Immunol 2020;146:1204-1208.e6.
23. Raffaele CGL, Messia V, Moneta G, Caiello I, Federici S, Pardeo M, et al. A patient with stimulator of interferon genes-associated vasculopathy with onset in infancy without skin vasculopathy. Rheumatology 2020;59:905-7.
24. Ma M, Mazumder S, Kwak H, Adams M, Gregory M. Case report: acute thrombotic microangiopathy in a patient with STING-associated vasculopathy with onset in infancy (SAVI). J Clin Immunol 2020;40:1111-5.
25. Rodero MP, Decalf J, Bondet V, Hunt D, Rice GI, Werneke S, et al. Detection of interferon alpha protein reveals differential levels and cellular sources in disease. J Exp Med 2017;214:1547-55.
26. Frémond M-L, Rodero MP, Jeremiah N, Belot A, Jeziorski E, Duffy D, et al. Efficacy of the Janus kinase 1/2 inhibitor ruxolitinib in the treatment of vasculopathy associated with TMEM173-activating mutations in 3 children. J Allergy Clin Immunol 2016;138:1752-5.
27. Sanchez GAM, Reinhardt A, Ramsey S, Wittkowski H, Hashkes PJ, Berkun Y, et al. JAK1/2 inhibition with baricitinib in the treatment of autoinflammatory interferonopathies. J Clin Invest 2018;128:3041-52.
28. Rice GI, Forte GMA, Szynkiewicz M, Chase DS, Aeby A, Abdel-Hamid MS, et al. Assessment of interferon-related biomarkers in Aicardi-Goutières syndrome associated with mutations in TREX1, RNASEH2A, RNASEH2B, RNASEH2C, SAMHD1, and ADAR: a case-control study. Lancet Neurol 2013;12:1159-69.
29. Fischer A, Antoniou KM, Brown KK, Cadranel J, Corte TJ, du Bois RM, et al. An official European Respiratory Society/American Thoracic Society research statement: interstitial pneumonia with autoimmune features. Eur Respir J 2015;46:976-87.
30. Crow YJ, Chase DS, Lowenstein Schmidt J, Szynkiewicz M, Forte GMA, Gornall HL, et al. Characterization of human disease phenotypes associated with mutations in TREX1, RNASEH2A, RNASEH2B, RNASEH2C, SAMHD1, ADAR, and IFIH1. Am J Med Genet A 2015;167A:296-312.
31. Wu Y, Zheng J. Jaccoud's arthropathy and psoriatic arthritis, a rare association. Rheumatol Int 2010;30:1081-3.
32. Santiago MB, Galvão V, Ribeiro DS, Santos WD, da Hora PR, Mota AP, et al. Severe Jaccoud's arthropathy in systemic lupus erythematosus. Rheumatol Int 2015;35:1773-7.
33. Shearer WT, Rosenblatt HM, Gelman RS, Oyomopito R, Plaeger S, Stiehm ER, et al. Lymphocyte subsets in healthy children from birth through 18 years of age: the Pediatric AIDS Clinical Trials Group P1009 study. J Allergy Clin Immunol 2003;112:973-80.
34. Dinwiddie R, Sharief N, Crawford O. Idiopathic interstitial pneumonitis in children: a national survey in the United Kingdom and Ireland. Pediatr Pulmonol 2002;34:23-9.
35. Clement A, ERS Task Force. Task force on chronic interstitial lung disease in immunocompetent children. Eur Respir J 2004;24:686-97.
36. Eloranta M-L, Franck-Larsson K, Lövgren T, Kalamajski S, Rönnblom A, Rubin K, et al. Type I interferon system activation and association with disease manifestations in systemic sclerosis. Ann Rheum Dis 2010;69:1396-402.
37. Christmann RB, Sampaio-Barros P, Stifano G, Borges CL, de Carvalho CR, Kairalla R, et al. Association of interferon- and transforming growth factor β-regulated genes and macrophage activation with systemic sclerosis-related progressive lung fibrosis. Arthritis Rheumatol 2014;66:714-25.
38. Warner JD, Irizarry-Caro RA, Bennion BG, Ai TL, Smith AM, Miner CA, et al. STING-associated vasculopathy develops independently of IRF3 in mice. J Exp Med 2017;214:3279-92.
39. Bouis D, Kirstetter P, Arbogast F, Lamon D, Delgado V, Jung S, et al. Severe combined immunodeficiency in stimulator of interferon genes (STING) V154M/wild-type mice. J Allergy Clin Immunol 2019;143:712-725.e5.
40. Luksch H, Stinson WA, Platt DJ, Qian W, Kalugotla G, Miner CA, et al. STING-associated lung disease in mice relies on T cells but not type I interferon. J Allergy Clin Immunol 2019;144:254-266.e8.
41. Motwani M, Pawaria S, Bernier J, Moses S, Henry K, Fang T, et al. Hierarchy of clinical manifestations in SAVI N153S and V154M mouse models. Proc Natl Acad Sci USA 2019;116:7941-50.
42. Melki I, Frémond M-L. Type I interferonopathies: from a novel concept to targeted therapeutics. Curr Rheumatol Rep 2020;22:32.
43. Hinks A, Marion MC, Cobb J, Comeau ME, Sudman M, Ainsworth HC, et al. Brief report: the genetic profile of rheumatoid factor-positive polyarticular juvenile idiopathic arthritis resembles that of adult rheumatoid arthritis. Arthritis Rheumatol 2018;70:957-62.
44. La Piana R, Uggetti C, Roncarolo F, Vanderver A, Olivieri I, Tonduti D, et al. Neuroradiologic patterns and novel imaging findings in Aicardi-Goutières syndrome. Neurology 2016;86:28-35.
45. Zhang X, Bogunovic D, Payelle-Brogard B, Francois-Newton V, Speer SD, Yuan C, et al. Human intracellular ISG15 prevents interferon-α/β over-amplification and auto-inflammation. Nature 2015;517:89-93.
46. Watkin LB, Jessen B, Wiszniewski W, Vece TJ, Jan M, Sha Y, et al. COPA mutations impair ER-Golgi transport and cause hereditary autoimmune-mediated lung disease and arthritis. Nat Genet 2015;47:654-60.
47. Deng Z, Chong Z, Law CS, Mukai K, Ho FO, Martinu T, et al. A defect in COPI-mediated transport of STING causes immune dysregulation in COPA syndrome. J Exp Med 2020;217:e20201045.
48. Mukai K, Ogawa E, Uematsu R, Kuchitsu Y, Uemura T, Waguri S, et al. Homeostatic regulation of STING by Golgi-to-ER membrane traffic. BioRxiv 2020. https://doi.org/10.1101/2020.05.20.107664.
49. Steiner A, Hrovat Schaale K, Prigione I, De Nardo D, Dagley LF, Yu C-H, et al. Activation of STING due to COPI-deficiency. BioRxiv 2020. https://doi.org/10.1101/2020.07.09.194399.
50. Rodero MP, Tesser A, Bartok E, Rice GI, Della Mina E, Depp M, et al. Type I interferon-mediated autoinflammation due to DNase II deficiency. Nat Commun 2017;8:2176.
51. Boulisfane-El Khalifi S, Viel S, Lahoche A, Frémond M-L, Lopez J, Lombard C, et al. COPA syndrome as a cause of lupus nephritis. Kidney Int Rep 2019;4:1187-9.

52. Cerboni S, Jeremiah N, Gentili M, Gehrmann U, Conrad C, Stolzenberg M-C, et al. Intrinsic antiproliferative activity of the innate sensor STING in T lymphocytes. J Exp Med 2017;214:1769-85.
53. Wu J, Chen Y-J, Dobbs N, Sakai T, Liou J, Miner JJ, et al. STING-mediated disruption of calcium homeostasis chronically activates ER stress and primes T cell death. J Exp Med 2019;216:867-83.
54. Wu J, Dobbs N, Yang K, Yan N. Interferon-independent activities of mammalian STING mediate antiviral response and tumor immune evasion. Immunity 2020;53:115-126.e5.
55. Haag SM, Gulen MF, Reymond L, Gibelin A, Abrami L, Decout A, et al. Targeting STING with covalent small-molecule inhibitors. Nature 2018;559:269-73.

ONLINE REPOSITORY

METHODS

Cohort of patients

Patients were recruited from institutions in France (Necker Hospital, Paris; Hospices Civils de Lyon, Lyon; Centre Hospitalier Universitaire de Montpellier, Montpellier; Centre Hospitalier Universitaire de Lille, Lille; Hôpital La Timone Enfants, Marseille), Monaco (Centre Hospitalier Princesse Grace), Belgium (University Hospitals Leuven, Leuven), Italy (Istituto Gaslini, Genoa; and Ospedale Pediatrico Bambino Gesù, Rome), Spain (Hospital Universitari Vall d'Hebron, Barcelona), Lebanon (Notre Dame De Secours University Hospital, Jbeil), and Australia (Lady Cilento Children's Hospital, Brisbane).

Thoracic imaging analyses

Computed tomography thoracic imaging was analyzed at 3 levels in each lung: upper thoracic region: above the aortic arch; mid-thoracic region: at the level of carina; lower thoracic region: at the confluence of the inferior pulmonary veins. Twelve items[E1] were assessed for each of the 6 studied areas: (1) Ground-glass opacity, (2) Consolidation, (3) Micronodules, (4) Interlobular septal thickening, (5) Intralobular lines, (6) Pleural thickening, (7) Paraseptal and centrolobular cyst, (8) Honeycombing, (9) Bronchiectasis, (10) Inflation, (11) Lung volumes, (12) Lymphadenopathies. Extension of the lesions (items 1, 2, 3, 4, 5, 7, and 8) was determined according to the rating scale below: 0: no lesion; 1: extension less than 25% of the studied area; 2: extension between 25% and 50% of the studied area; 3: extension between 50% and 75% of the studied area; 4: extension more than 75% of the studied area.

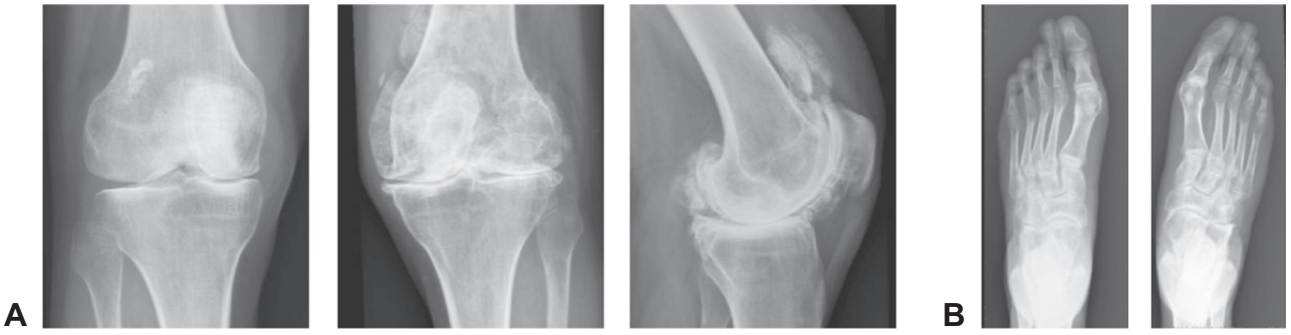

FIGURE E1. Joint involvement observed in P3. **A**, Conventional X-rays of the knees (anteroposterior view for both knees and lateral view of the left knee) of P3, at the age of 33 years, showing bilateral joint space narrowing, a subchondral cyst (geode) of the left medial femoral condyle, and articular and periarticular ossifications on the left knee that were evocative of calcinosis. **B**, Conventional anteroposterior X-ray of the feet of P3 performed at the age of 33 years demonstrating joint space narrowing and bone demineralization.

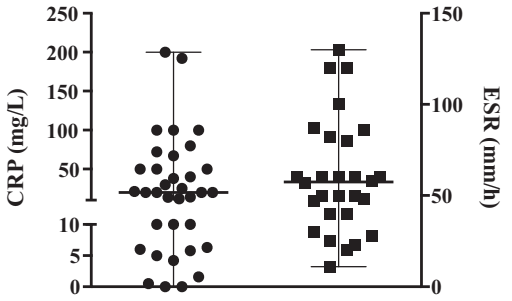

FIGURE E2. Systemic inflammation markers observed in the patients. Levels of C-reactive protein (CRP, normal <6 mg/L) and erythrocyte sedimentation rate (ESR, normal <20 mm/h) recorded in 20 patients of the cohort (not assessed in P6). Minimal and maximal values of CRP and ESR during the course of the disease or, if not available, the values at screening were included. The median CRP was at 20 mg/L (range, 0-200 mg/L) and the median ESR was 57 mm/h (range, 11-130 mm/h).

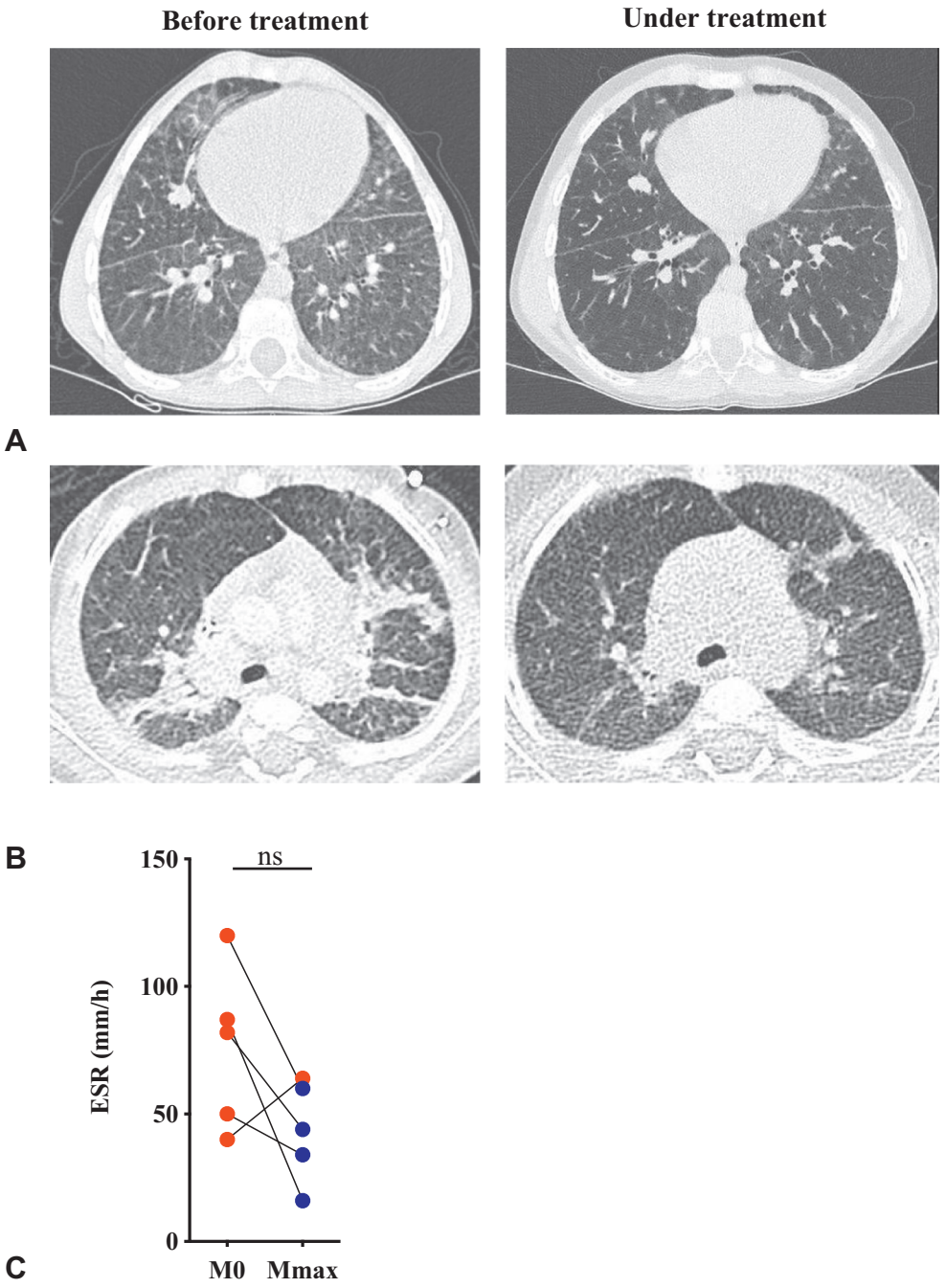

FIGURE E3. Chest computed tomography (CT) imaging performed in P9 and P16, and erythrocyte sedimentation rate before and during treatment with ruxolitinib. **A**, Chest CT scan of P9 performed at the age of 7.5 years showed bilateral alveolar and interstitial disease with ground-glass lesions, interlobular septa thickening, and cystic lesions, associated with features of fibrosis (traction bronchiectasis and honeycombing). After 26 months of treatment with ruxolitinib, the ground-glass lesions were less marked and fibrosis stabilized, although honeycombing slightly increased. **B**, Chest CT scan of P16 performed at the age of 7 months showed bilateral subpleural consolidations predominantly located in the posterior thoracic region associated with some microcysts and traction bronchiectasis. After 12 months of treatment with ruxolitinib, the consolidation lesions decreased, whereas fibrotic lesions remained unchanged. **C**, Erythrocyte sedimentation rate (ESR) values (normal $<$20 mm/h) recorded in 5 patients at screening (M0) and at maximal follow-up (Mmax). A reduction of at least 20% in the values of ESR of Mmax as compared with M0 is represented in blue. Raised levels of ESR before treatment or decreased less than 20% or increased at Mmax are pictured in red. Median level of ESR decreased from 82 mm/h (interquartile range [IQR], 45-103.5 mm/h) at M0 to 44 mm/h (IQR, 25-64 mm/h) at Mmax (nonsignificant [ns], using the Wilcoxon test).

TABLE E1. Characteristics of the patients with mutations in *STING1*

	P1	P2*	P3	P4*,†	P5	P6‡	P7	P8	P9	P10	P11	P12	P13	P14	P15	P16	P17	P18	P19	P20	P21
Age at onset	1	13	13	NR	1	5	0.4	0.2	0.5	Birth	Birth	1	0.75	2	3	Birth	0.7	0.3	Birth	0.5	1.5
Status (age)	A (3)	D (29)	A (33)	A (65)	A (11)	D (34)	A (14)	A (8)	A (7)	A (2)	D (14)	A (12)	A (18)	A (8)	A (8)	A (0.6)	A (10)	A (7)	A (2)	A (1.8)	A (23)
Gender	F	M	M	M	M	F	M	M	M	M	M	F	M	F	M	M	F	F	F	F	F
Mutation of *STING1*	p.V155M	p.V155M	p.V155M	p.V155M	p.V155M	p.V155M	p.V155M	p.V147M	p.N154S	p.N154S	p.N154S	p.V155M	p.C206Y	p.R281Q	p.V155M	p.V155M	p.V155M	p.R281Q	p.N154S	p.V155M	p.V155M
Inheritance	AD	AD	AD	ND	AD	ND	*De novo*	*De novo*	*De novo*	ND	ND	*De novo*	*De novo*	*De novo*	*De novo*	*De novo*	*De novo*	*De novo*	*De novo*	*De novo*	ND
Clinical features																					
Onset symptoms	FTT	Arthritis & fevers	Arthritis & fevers	FTT	Lung	Lung	Lung	Skin	Skin & lung	Skin & lung & fevers	Skin & FTT & arthritis	Lung	Skin	Arthritis	Skin & fevers	CID & lung	Skin & fevers	Lung	Skin & lung	Lung	Skin & FTT
FTT	+	+	+	+	+	NR	+	+	+	+	+	+	-	-	+	+	-	+	-	-	+
Height < −3SD	+	-	-	-	-	NR	-	+	-	+	+	-	-	-	-	-	-	-	-	-	-
Fevers/SI	+/+	+§/+	+§/+	-/+	+/+	NR	-/+	+§/+	+/+	+/+	+/+	-/+	-/+	+/+	+/+	+/+	+§/+	-/+	+/+	+/+	-/+
Skin status																					
Rash	+	+	+	-	+	+	+	+	+	+	+	-	+	+	+	-	+	+	+	+	+
Ulcers	-	+	+	-	+	-	-	+	+	+	+	-	+	-	+	-	-	-	+	-	+
Loss of tissue	-	-	-	-	-	-	-	+	+	+	+	-	+	-	-	-	-	-	-	-	-
Nasal perforation	-	-	-	-	-	-	-	+	+	-	+	-	-	-	-	-	-	-	-	-	-
Lung disease																					
ILD	+	+	+	+	+	+	+	+	+	+	+	+	-	+	+	+	+	+	+	+	+
Lung fibrosis	+	+	+	+	+	+	+	-	+	-	+	+	-	+	-	+	+	+	-	+	+
End-stage pulmonary failure	-	-	-	-	+	+	+	-	-	-	+	+	-	-	-	-	-	+	-	-	-
Joint and muscle status																					
Arthritis	-	+	+	-	-	-	-	-	+	-	+	+	-	+	+	-	-	-	-	-	-
Myositis	-	-	-	-	-	-	-	-	+	-	-	-	-	-	-	-	-	-	-	-	-
Neurological status																					
Symptoms	-	-	-	-	-	-	-	-	-	+	+	-	-	-	-	-	-	-	-	-	-
ICC	-	NR	NR	NR	-	NR	-	+	NR	+	+	-	-	-	NR	-	NR	-	NR	NR	-
Infections																					
	-	+	-	-	+	-	-	-	-	-	+	-	+	-	-	-	-	+	-	-	-
Other organ involvement																					
											Heart	Eye, heart					Kidney	Liver			Kidney
Autoantibodies																					
ANA	+	+	+	+	-	Transient	+	Transient	+	-	+	+	-	+	+	+	Transient	-	-	+	-
Anti-DNA	Transient	-	-	-	+	NR	-	Transient	-	-	-	Transient	NR	-	-	-	-	+	-	-	-
ANCA	+	+	+	+	-	+	+	+	-	-	+	+	-	+	+	-	+	+	+	-	Transient
RF	+	+	+	+	-	+	-	-	-	+	Transient	+	-	+	+	-	+	-	-	NR	NR
Treatments and procedures																					
Steroids‖	+/+	+/-	+/-	-/-	+/+	NR/NR	+/+	+/-	+/-	+/-	+/-	+/+	-/-	+/+	+/+	-/-	+/+	+/+	+/-	-/+	+/-
DMARDs	MMF	MTX, HCQ, CyA, lefluno-mide	MTX, HCQ, CyA	-	HCQ	NR	HCQ	HCQ, MMF, MTX, COL, aspirin	MMF, AZA, CyA, TAC, HCQ	-	Aspirin, COL, CyA	COL, CyA, MMF, HCQ, NSAIDs	Aspirin	-	AZA	-	AZA	MTX	-	HCQ	MMF, HCQ, MTX

(continued)

TABLE E1. *(Continued)*

	P1	P2*	P3	P4*,†	P5	P6‡	P7	P8	P9	P10	P11	P12	P13	P14	P15	P16	P17	P18	P19	P20	P21
Biologics	RTX	ADA, ETN, RTX	ETN	-	-	NR	-	RTX	ANR, TOC	-	-	ANR, TOC	-	ANR, ETN, TOC	-	-	ETN	IFX	-	-	RTX
JAK inhibitors initiated after end point of data collection	+	/	+	+	+	/	+	+	+	-	/	+	+	+	+	+	+	+	+	+	+
Others						Lung Tx	¶					¶									

Ages are given in years. SI refers to increased inflammatory markers.

+, Present; -, absent; *A*, alive; *AD*, autosomal dominant; *ADA*, adalimumab; *ANA*, antinuclear antibodies; *ANCA*, antineutrophil cytoplasmic antibodies; *ANR*, anakinra; *anti-DNA*, anti−double-stranded DNA antibodies; *AZA*, azathioprine; *COL*, colchicine; *CyA*, cyclosporine A; *D*, deceased; *DMARDs*, disease-modifying antirheumatic drugs; *ETN*, etanercept; *F*, female; *FTT*, failure to thrive; *HCQ*, hydroxychloroquine; *ICC*, intracranial calcification; *IFX*, infliximab; *ILD*, interstitial lung disease; *JAK*, Janus kinase; *M*, male; *MMF*, mycophenolate mofetil; *MTX*, methotrexate; *ND*, not determined; *NR*, not recorded; *NSAIDs*, nonsteroidal anti-inflammatory drugs; *P*, patient; *RF*, rheumatoid factor; *RTX*, rituximab; *SD*, standard deviation; *SI*, systemic inflammation; *TAC*, tacrolimus; *TOC*, tociluzimab; *Tx*, transplantation.

*Father of P1.

†Grandfather of P1, father of P2 and P3.

‡Mother of P5.

§During infancy.

‖Prednisone/pulse of methylprednisolone.

¶Patients programmed for lung transplantation after the end point of data collection.

TABLE E2. Genetic findings

	Mutation of *STING1*	Inheritance
P1	Het: c.463G>A/p.V155M	AD
P2 (father of P1)	Het: c.463G>A/p.V155M	AD
P3 (uncle of P1)	Het: c.463G>A/p.V155M	AD
P4 (grandfather of P1)	Het: c.463G>A/p.V155M	Unknown*
P5	Het: c.463G>A/p.V155M	AD
P6 (mother of P5)	Het: c.463G>A/p.V155M	Unknown*
P7	Het: c.463G>A/p.V155M	*De novo*
P8	Het: c.439G>A/p.V147M	*De novo*
P9	Het: c.461G>A/p.N154S	*De novo*
P10	Het: c.461G>A/p.N154S	Unknown*
P11	Het: c.461G>A/p.N154S	Unknown*
P12	Het: c.463G>A/p.V155M	*De novo*
P13	Het: c.617G>A/p.C206Y	*De novo*
P14	Het: c.842G>A/p.R281G	*De novo*
P15	Het: c.463G>A/p.V155M	*De novo*
P16	Het: c.463G>A/p.V155M	*De novo*
P17	Het: c.463G>A/p.V155M	*De novo*
P18	Het: c.842G>A/p.R281G	*De novo*
P19	Het: c.461G>A/p.N154S	*De novo*
P20	Het: c.463G>A/p.V155M	*De novo*
P21	Het: c.463G>A/p.V155M	Unknown*

AD, Autosomal dominant; *Het*, heterozygous; *P*, patient.
*DNA from parents was not available to determine inheritance.

TABLE E3. Pulmonary function tests in the patients

	First PFT	Last PFT available
P1	*3y1m* Hyperinflation (FRC 160%) Normal DL_{CO}	*3y9m* Hyperinflation (FRC 188%) Normal DL_{CO}
P5	*9y4m* Restrictive pattern Hyperinflation Reduced DL_{CO}	*11y6m* Restrictive pattern Hyperinflation Reduced DL_{CO}
P7	*9y* Restrictive pattern Reduced DL_{CO}	*14y* Restrictive pattern Hyperinflation
P8	NR	*8y4m* Mild restrictive defect No hyperinflation
P9	*4y11m* Decreased VC	*7y8m* Decreased VC
P12	NR	*12y6m* Restrictive pattern Hyperinflation
P13	*15y* Normal	*17y* Mild restrictive defect No hyperinflation Reduced DL_{CO}
P14	*4y9m* Decreased VC	*8y1m, last pulse of steroids 6m before* Decreased VC Hyperinflation Normal DL_{CO}
P15	*7y* NA*	*8y* Decreased VC Hyperinflation Reduced DL_{CO}
P16	NA†	NA†
P17	*8y* No hyperinflation Reduced DL_{CO} at 57%	*9y* Decreased VC
P18	NA	*7y* Decreased VC No hyperinflation DL_{CO} non collaborative
P19	NA†	NA†
P20	NA†	NA†
P21	NR	*22y* Restrictive pattern Hyperinflation Reduced DL_{CO}

A restrictive spirometric pattern was defined as a decreased total lung capacity (TLC) above 80% of the predicted values for age and height. A hyperinflation pattern was defined as an increased RV/TLC above 120% of the predicted values for age and height. A diffusing capacity of the lungs for carbon monoxide (DL_{CO}) below 80% of the predicted value was considered abnormal.

FRC, Functional residual capacity; *m*, month; *NA*, not assessed; *NR*, not recorded; *P*, patient; *PFT*, pulmonary function test; *RV*, residual volume; *VC*, vital capacity; *y*, year.

*Nonassessed because of patient noncompliance.

†Too young to perform PFT.

TABLE E4. Chest computed tomography findings in the patients at screening

	P1	P3	P4	P7	P8	P9	P11	P12	P13	P14	P15	P16	P17	P18	P20	P21
Age (y)	3	33	65	6	0.5	7	11	4.5	15	5	6	0.6	10	3.1	1.75	23
Lesions observed																
Ground-glass	++	+	+	-	+++	+++	++	+++	-	+	+	+	+	++	++	+
Consolidation	+	-	+	-	-	-	-	-	-	+	-	+	-	+	+	-
Micronodules	-	-	-	-	-	-	-	-	-	-	-	-	-	-	-	-
Interlobular septal thickening	++	+	+	+	-	++	++	+++	-	+++	+	+	+	+	++	+
Intralobular lines	+++	+	+++	+++	-	+++	++	+	-	++	+++	+	++	+	++	++
Cysts	+ (μ & M)	+ (μ)	+++ (μ & M)	+ (M)	-	+ (μ)	+ (μ)	+ (M)	-	-	-	+ (μ)	+ (μ)	-	+ (μ)	++ (μ)
Honeycombing	-	-	++	+	-	+	-	-	-	-	-	-	+	-	+	++
Chest CT score	54	16	66	38	20	55	43	56	0	38	36	20	27	30	54	47
Other characteristics																
Pleural thickening	Irregular (fissures)	Irregular (fissures)	Irregular (fissures)	Smooth (fissures) Triangular subpleural opacities	No	Irregular (fissures)	Irregular	Irregular (fissures)	Irregular (fissures)	Irregular (fissures)	Irregular	Irregular (fissures)	Irregular (fissures)	Irregular (fissures	Irregular (fissures)	Irregular (fissures)
Traction bronchiectasis	Scattered	Few	Few	No	No	Few	Few	No	No	Scattered	No	Few	No	Few	Few	Yes
Overinflation	No	No	No	Yes*	No	Yes	No	No	No	No	No	Yes	Yes	Yes	Yes	Yes
Lung volumes	Decrease (L)	N	Decrease	Decrease	N	N	Decrease (L)	N	N	N	N	N	N	Increase	Decrease	N
Lymphadenopathies	+++	-	-	NA	NA	++	-	-	-	-	+++	+++	-	-	+++	
Comment	Diffuse TBB	Asym. lobar retractions	/	/	/	/	/	/	/	/	/	/	/	/	/	/
Conclusion																
ILD	Yes	Yes	Yes	Yes	Yes	Yes	Yes	Yes	No	Yes	Yes	Yes	Yes	Yes	Yes	Yes
Fibrosis	Yes	Yes	Yes	Yes	No	Yes	Yes	No	No	Yes	No	Yes	Yes	Yes	Yes	Yes

Rating:

Extension of 7 lesions—ground-glass opacities, consolidations, micronodules, interlobular septal thickening, intralobular lines, cysts, honeycombing—was graded according to this rating scale: 0 = -; 1-8 = +; 9-16 = ++; 17-24 = +++. The sum of the scores of these 7 items (range, 0-24) yields the chest CT score (range, 0-168).

"Lymphadenopathies" was graded according to the following rating scale: Absence = -; Unilateral = +; Bilateral = ++; Diffuse = +++.

The presence of honeycombing and/or traction bronchiectasis and/or decreased lung volume radiologically defined fibrosis.

Asym., Asymmetrical; *CT*, computed tomography; *ILD*, interstitial lung disease; *L*, left lung; *μ*, microcysts of subpleural localization or along the septa; *M*, macrocysts; *N*, normal; *NA*, not assessed; *P*, patient; *TBB*, thickening of the bronchovascular bundles; *y*, year.

*Overinflation could be explained by past surgical history.

TABLE E5. Chest computed tomography findings in P7 and P12

	P7	P7	P7	P12	P12
Age (y)	6	12.5	14	4.5	12
Clinical respiratory status	Tachypnoea Dyspnea on exertion	Tachypnoea Dyspnea at rest Nocturnal 02 PH	Tachypnoea Dyspnea at rest Continuous 02 Increased PH	Tachypnoea Dyspnea on exertion	Tachypnoea Increased dyspnea on exertion (daily activities) Nocturnal 02
Lesions					
Ground-glass	-	+	+	+++	+++ (stable)
Consolidation	-	-	+	-	-
Micronodules	-	-	-	-	-
Interlobular septal thickening	+	+ (stable)	+ (stable)	+++	++
Intralobular lines	+++	+++ (stable)	+++ (stable)	+	+ (stable)
Cysts	+ (M)	++ (M)	+++ (M)	+ (M)	+++ (μ & M)
Honeycombing	+	++	+++	-	++
Chest CT score	38	57	75	56	72
Other characteristics					
Pleural thickening	Smooth (fissures) & triangular subpleural opacities	Stable	Stable	Irregular (fissures)	Irregular (fissures) & triangular subpleural opacities
Traction bronchiectasis	No	No	Few	No	Few
Overinflation	Yes*	Yes*	Yes*	No	No
Lung volumes	Decrease	Further decrease	Further decrease	N	N
Lymphadenopathies	NA	NA	NA	-	-
Comment	/	/	Dilation of the pulmonary arteries	/	/
Conclusion					
ILD	Yes	Increase	Increase	Yes	Increase
Fibrosis	Yes	Increase	Increase	No	Yes

Rating:
Extension of 7 lesions—ground-glass opacities, consolidations, micronodules, interlobular septal thickening, intralobular lines, cysts, honeycombing—was graded according to this rating scale: 0 = -; 1-8 = +; 9-16 = ++; 17-24 = +++. The sum of the scores of these 7 items (range, 0-24) yields the chest CT score (range, 0-168).
"Lymphadenopathies" was graded according to the following rating scale: Absence = -; Unilateral = +; Bilateral = ++; Diffuse = +++.
The presence of honeycombing and/or traction bronchiectasis and/or decreased lung volume radiologically defined fibrosis.
CT, Computed tomography; *ILD*, interstitial lung disease; *μ*, microcysts of subpleural localization or along the septa; *M*, macrocysts; *N*, normal; *NA*, not assessed; *02*, oxygen therapy; *P*, patient; *PH*, pulmonary hypertension; *y*, year.
*Inflation could be explained by past surgical history.

TABLE E6. Bronchoalveolar lavage fluid analysis in patients with mutations in *STING1*

	Age (y)	No. of cells/mm^3	% of Mφ	% of Ly	% of neutrophil PMNs	Microbiology	Conclusion
P1	2.5	1100	12	3	85	–	Neutrophilic alveolitis
P2	28	NR	NR	NR	NR	*Aspergillus fumigatus*	Aspergillosis
P3	17	NR	NR	35	55	–	Mixed alveolitis with predominance of neutrophils
P7	1	1800	62	16	22	–	Mixed lymphocytic and neutrophilic alveolitis
P8	0.5	3400	30	55	5	–	Lymphocytic alveolitis
P9	1	NR	40	40	20	–	Mixed alveolitis with predominance of lymphocytes
P11	4	1000	72	14	14	–	Mixed alveolitis
P12	3	NR	20	10	56	–	Neutrophilic alveolitis
P14	4.8	850	70	28	2	–	Lymphocytic alveolitis
P16	0.6	190	60	22	18	–	Normal cellularity but excess of lymphocytes and PMN
P18	3 and 9	NR	59/26	10/12.5	31/24.5	*Pseudomonas aeruginosa*	Neutrophilic alveolitis
P20	1.8	720	31	20	45	Streptococcus alpha-hemolytic, *Pseudomonas aeruginosa*	Mixed lymphocytic and neutrophilic alveolitis
P21	3	NR	NR	NR	NR	NR	Alveolar hemorrhage

Ly, Lymphocytes; *Mφ*, macrophages; *NR*, not recorded; *P*, patient; *PMNs*: polymorphonuclear cells; *y*, year.

TABLE E7. Chest computed tomography findings in the patients of cohort at screening and at maximal follow-up

	P1	P1	P8	P8	P9	P9	P14	P14	P16	P16
Age (y)	4	7	8.5	11	7.5	10	7.5	9	0.6	1.5
Follow-up (m)	0	36	0	35	0	26	-6*	12	0	12
Lesions observed										
Ground-glass	++	+	NA†	NA† (stable)	+++	++	++	++ (decrease)	+	+ (stable)
Consolidation	+	-	-	-	-	-	+	-	+	+ (decrease)
Micronodules	-	-	-	-	-	-	-	-	-	-
Interlobular septal thickening	++	++ (increase)	-	-	++	++ (stable)	+++	++ (decrease)	+	+ (stable)
Intralobular lines	+++	+++ (stable)	+	+ (decrease)	+++	+++ (stable)	++	++ (stable)	+	+ (stable)
Cysts	++ (μ & M)	++ (stable)	+ (μ)	+ (stable)	+ (μ)	+ (stable)	-	-	+ (μ)	+ (stable)
Honey combing	+	+ (stable)	-	-	+	+ (stable)	-	-	-	-
Chest CT score	54	49	NA†	NA†	55	48	48	37	20	15
Pleural thickening	Irregular (fissures) Linear atelectasis	Increase Decrease	Irregular (fissures)	Stable	Irregular (fissures)	Stable	Irregular (fissures)	Stable	Irregular (fissures)	Stable
Traction bronchiectasis	Scattered	Stable	No	No	Few	Stable	Scattered	Stable	Few	Stable
Inflation	No	No	No	No	Yes	Stable	No	No	Yes	No
Lung volumes	Decrease (L)	Partial recovery of the L volume	N	N	N	N	N	N	N	N
Lymphadenopathies	+++	+++	NA	NA	++	-	-	-	+++	+++
Comment	Diffuse TBB	Idem	/	/	/	/	/	/	/	/
Conclusion										
ILD	Yes	Decrease	Yes	Decrease	Yes	Decrease	Yes	Decrease	Yes	Decrease
Fibrosis	Yes	Stable	No	No	Yes	Stable	Yes	Stable	Yes	Stable

Rating:

Extension of 7 lesions—ground-glass opacities, consolidations, micronodules, interlobular septal thickening, intralobular lines, cysts, honeycombing—was graded according to this rating scale: 0 = -; 1-8 = +; 9-16 = ++; 17-24 = +++. The sum of the scores of the 7 items (range, 0-24) above yields the chest CT score (range, 0-168).

"Lymphadenopathies" was graded according to the following rating scale: Absence = -; Unilateral = +; Bilateral = ++; Diffuse = +++.

The presence of honeycombing and/or traction bronchiectasis and/or decreased lung volume radiologically defined fibrosis.

CT, Computed tomography; *ILD*, interstitial lung disease; *L*, left lung; *μ*, microcysts of subpleural localization or along the septa; *m*, month; *M*, macrocysts; *N*, normal; *NA*, not assessed; *P*, patient; *TBB*, thickening of the bronchovascular bundles; *y*, year.

*Before last pulse steroid therapy before initiation of ruxolitinib.

†The precise extension of the ground-glass lesions was not assessable.

REFERENCE

E1. Hansell DM, Bankier AA, MacMahon H, McLoud TC, Müller NL, Remy J, Fleischner Society. glossary of terms for thoracic imaging. Radiology 2008;246: 697-722.